Special Issue: WAFR 2022

The International Journal of Robotics Research
2023, Vol. 0(0) 1–23

DOI: 10.1177/02783649231188740
journals.sagepub.com/home/ijr

Abstracting road traffic via topological braids: Applications to traffic flow analysis and distributed control

Christoforos Mavrogiannis[1,2], Jonathan A DeCastro[3] and Siddhartha S Srinivasa[1]

Abstract

Despite the structure of road environments, imposed via geometry and rules, traffic flows exhibit complex multiagent dynamics. Reasoning about such dynamics is challenging due to the high dimensionality of possible behavior, the heterogeneity of agents, and the stochasticity of their decision-making. Modeling approaches learning associations in Euclidean spaces are often limited by their high sample complexity and the sparseness of available datasets. Our key insight is that the structure of traffic behavior could be effectively captured by lower-dimensional abstractions that emphasize critical interaction relationships. In this article, we abstract the space of behavior in traffic scenes into a discrete set of interaction modes, described in interpretable, symbolic form using topological braids. First, through a case study across real-world datasets, we show that braids can describe a wide range of complex behavior and uncover insights about the interactivity of vehicles. For instance, we find that high vehicle density does not always map to rich mixing patterns among them. Further, we show that our representation can effectively guide decision-making in traffic scenes. We describe a mechanism that probabilistically maps vehicles' past behavior to modes of future interaction. We integrate this mechanism into a control algorithm that treats navigation as minimization of uncertainty over interaction modes, and investigate its performance on the task of traversing uncontrolled intersections in simulation. We show that our algorithm enables agents to coordinate significantly safer traversals for similar efficiency compared to baselines explicitly reasoning in the space of trajectories across a series of challenging scenarios.

Keywords

Topological braids, multiagent systems, distributed control, topological data analysis, traffic flow analysis, autonomous driving

1. Introduction

Road environments give rise to complex multiagent behavior involving a variety of actors including vehicles, pedestrians, and cyclists. This behavior is regulated through the spatial structure of the environment (i.e., crosswalks, sidewalks, dedicated lanes), technological tools (e.g., traffic lights, turn signals), and laws (e.g., right of way, no right turn on red). However, in practice, agent-to-agent variability, local customs, and inconsistencies in the placement of signs and traffic lights (Patil and Pawar 2016) result in unstructured motion that requires on-the-fly coordination to avoid dangerous situations.

While humans are able to use subtle social cues to coordinate even in challenging multiagent encounters quickly and effectively, engineering such mechanisms on autonomous vehicles requires a holistic scene understanding which is challenging to achieve. Under assumptions like full state observability, rationality, and purely kinematic state representations, recent work has proposed data-driven mechanisms for behavior prediction and planning that incorporate models of multiagent coordination (Sadigh et al. 2016; Tian et al. 2022; Bouton et al. 2017; Roh et al. 2020; Hsu et al. 2018; Salzmann et al. 2020; Gadepally et al. 2017; DeCastro et al. 2020; Mavrogiannis et al. 2022a). A common challenge for these mechanisms is their data dependence: dataset size and richness greatly affect the quality of exhibited behavior. While acquiring massive traffic datasets is relatively straightforward given appropriate infrastructure and capital, ensuring high quality of datasets is less trivial: the high dimensionality of the space of exhibited behavior, the heterogeneity of agents, and the complexity of the context

[1]Paul G. Allen School of Computer Science & Engineering, University of Washington, Seattle, WA, USA
[2]Department of Robotics, University of Michigan, Ann Arbor, MI, USA
[3]Toyota Research Institute, Cambridge, MA, USA

Corresponding author:
Christoforos Mavrogiannis, Department of Robotics, University of Michigan, Room 3248, Ford Motor Company Robotics Building 2505 Hayward St, Ann Arbor, MI 48109-2106, USA.
Email: cmavro@umich.edu

complicate the analysis and evaluation of datasets. For instance, it can be challenging to understand the support of a dataset over the space of behavior because our understanding of that space is incomplete. While recent deep learning architectures can discover behavior patterns in unsupervised or self-supervised ways (Kuefler et al. 2017; Bansal et al. 2018; Chen et al. 2019; Kebria et al. 2019), this comes at the cost of high sample complexity and lack of model interpretability.

Our goal is to assist in the evaluation of traffic datasets and enhancing the interpretability of architectures for inference and control by employing mathematical tools that allow the abstraction and characterization of complex multiagent behavior. While recent work has proposed tools for characterizing multiagent behavior probabilistically (Tolstaya et al. 2021; Liebenwein et al. 2020; DeCastro et al. 2020; Mavrogiannis et al. 2022a), there is little treatment of the underlying *semantic representations of the state* of that behavior and most require domain knowledge to reason over trajectories. The high dimensionality of conventionally employed Euclidean space representations may make it challenging to detect critical interaction events involving multiple agents, like overtaking or merging. Our key insight is that many of these events exhibit *topological* signatures that may be captured in a formal and interpretable fashion using tools from algebraic topology. To highlight the utility of topological reasoning and contrast with other related approaches, we demonstrate that our analysis requires no explicit domain knowledge or priors (e.g., language, rules of the road, etc.) for meaningful semantic representations to emerge.

In this article, we abstract multiagent traffic behavior as a topological braid (Artin 1947), a compact and interpretable topological object with symbolic and geometric descriptions. First, we adapt the braid representation of Mavrogiannis and Knepper (2019) to structured domains like traffic scenes through a rigorous mathematical presentation. We then study its computational properties, discussing its computational compression and how an index of topological complexity acting on braids (Dynnikov and Wiest 2007) may capture the interactivity of the behavior exhibited in a traffic scene. Through an extensive empirical study on multiple complex real-world traffic datasets of behaviors in intersections and roundabouts (Bock et al. 2020, 2021; Krajewski et al. 2020), we demonstrate that our braided representation may succinctly summarize real-world traffic behavior and characterize its complexity. Our analysis uncovers a counterintuitive phenomenon in commonly used datasets: in the majority of scenes, a few simple braids dominate, indicating a low degree of interaction despite the majority of scenes having high traffic density (a usual metric for dataset richness). This demonstrates the merit of topological reasoning in providing valuable insights for the design and benchmarking of data-driven frameworks for prediction and planning, the evaluation and generation of driving datasets, as well as the analysis and design of road networks.

To further emphasize the value of our representation for online inference and control, we also consider a task of navigating at an uncontrolled, four-way street intersection (Najm et al. 2007) among multiple non-communicating agents. Note that solutions requiring explicit coordination protocols (e.g., first-come-first-serve traversals (Khayatian et al. 2020), connected-vehicle schemes (Bian et al. 2020), or implicit coordination mechanisms (e.g., game-theoretic reasoning that assumes knowledge of agents' objectives) (Cleac'h et al. 2020) fall outside of our scope; we are interested in a setting involving no prior coordination, giving rise to challenging decision-making encounters. We show that the spatial structure of the environment and the traffic rules, coupled with the assumed rationality of agents, tend to collapse multiagent behavior to a discrete set of *modes*. We show that these modes can be represented as topological braids which can form the basis for probabilistic inference of future multiagent behavior. We integrate this mechanism into an optimization-based reactive control algorithm which treats navigation as uncertainty reduction over modes. Through an ablation study over a series of simulation scenarios, we demonstrate that our algorithm enables more effective coordination (reflected in significantly lower collision rates) compared to baselines reasoning directly over Euclidean-space trajectories (Section 6). This observation suggests that incorporating symbolic reasoning about future interactions (in the form of topological features) in the decision-making process may yield proactive detection of critical interaction events unfolding in complex traffic scenes.

1.1. Contributions

In prior work, we proposed a framework based on the formalism of topological braids for abstracting multiagent traffic behavior and characterizing its complexity using topological braids (Mavrogiannis et al. 2022c). Based on this representation, we developed a control framework that treats navigation in traffic scenes as inference over a space of interaction primitives, represented as topological braids (Mavrogiannis et al. 2023). This paper unifies and extends these works by contributing:

- A comprehensive review of the literature, discussing how our work relates to recent work on modeling, prediction, and control for applications in driving domains, as well as work on the use of topological representations for robotics and multiagent systems.
- Analysis of an additional driving dataset using our topological analysis framework (Mavrogiannis et al. 2022c). In particular, we look at the uniD dataset (Bock et al. 2021), containing traffic episodes collected at an intersection at the RWTH Aachen University in Germany. We abstract these episodes as braids and

characterize the interaction complexity of its traffic flows.
- New simulations demonstrating our control framework (Mavrogiannis et al. 2023) on three new intersection scenarios, involving turns and aggressive agents. These scenarios demonstrate the robustness of our framework in handling different types of interactions and mixed traffic with heterogeneous agents.
- An extended discussion of the value and open challenges underlying the use of topological representations for analysis, reasoning, and control in traffic scenes.

2. Related work

We review relevant work from multiagent interaction modeling, multiagent coordination, model validation for driving domains, and applications of algebraic topology to robotics.

2.1. Modeling interaction in traffic scenes

The topic of modeling the complex multiagent interactions unfolding in traffic scenes has recently received considerable attention (Wang et al. 2022a).

Much of the recent work on behavior prediction and decision-making for autonomous driving applications has leveraged discrete, semantic representations of multiagent traffic behavior. For instance, Wang et al. (2022b) classify discrete driving styles using a variant of hidden Markov models (HMM). Gadepally et al. (2017) also use HMM to estimate long-term driver behaviors from a sequence of discrete decisions. Others, such as Konidaris et al. (2018) and Shalev-Shwartz et al. (2016), propose using learned symbolic representations for high-level planning and collision avoidance, via a hierarchical options model. Others have explored temporal logic to semantically cluster and classify trajectories. For instance, Bombara et al. (2016) build a decision-tree classifier over trajectories from signal temporal logic (STL), while Vazquez-Chanlatte et al. (2017) employ time-series reasoning techniques to cluster trajectories, and Mohammadinejad et al. (2020) adopt an enumerative time-series clustering approach to construct STL formulas abiding by Occam's razor, where simple-to-explain clusterings are preferred.

Deep learning approaches have also been explored to reason over interactions between agents. Tang and Salakhutdinov (2019) learn latent representations of multiagent interaction in traffic scenes and use them as sample high-probability modes of future multiagent trajectories. Luo et al. (2022) learn end-to-end models of trajectory prediction leveraging pairwise interaction graphs to model interaction across agents. Roh et al. (2020) formalize pairwise interaction using a notion of topological invariance and define multimodality as a distribution over multiagent interaction primitives which is used to condition multiagent trajectory prediction for decentralized navigation. Yao et al. (2017) learn features that operate over a fixed window to learn space- and time-invariant properties of trajectories for clustering. Yue et al. (2019) also learn latent representations and improve and generalize clustering performance by employing feature augmentation.

Overall, we observe two key trends in this space: representations that might not exhibit semantically meaningful and consistent interpretations of observed interactions, and representations that incorporate domain knowledge or priors to elicit such semantic meaning. In this work, we harness topological representations to provide semantic meaning without imposing explicit domain knowledge or task-specific information. In fact, the topological abstraction of the behavior enables a formal specification of the domain structure, which we exploit in case studies on analysis (Section 4) and reasoning (Section 6).

2.2. Model validation in autonomous driving

A relevant body of work focuses on verification tools to support the development of inference and decision-making mechanisms.

Tian et al. (2022) model traffic at unsignalized intersections using tools from game theory and propose a verification testbed for navigation algorithms. Liebenwein et al. (2020) propose a framework for safety verification of driving controllers based on compositional and contract-based principles. Hsu et al. (2018) investigate how velocity signals generated by Markov decision processes affect interaction dynamics at intersections. DeCastro et al. (2020) construct a representation of multi-vehicle interaction outcomes based on latent parameters using a generative model. Li et al. (2023) develop a validation framework that systematically generates high-risk multiagent scenarios and verifies system properties based on specifications formulated in linear temporal logic. Tolstaya et al. (2021) propose a probabilistic *Interactivity* score based on the formalism of mutual information that enables the identification of interesting interactive scenarios for training generative models. Ding et al. (2021) propose a means to learn a generative model and sample from it using semantic structure capturing domain-specific properties embedded within the model.

Our work is complementary to the aforementioned methods, contributing topological tools for summarizing traffic scenarios and characterizing their complexity. Techniques from topological data analysis (Ghrist 2007) have offered valuable insights in many real-world domains (Chazal and Michel 2021). While there has been prior work on the use of methods from topological data analysis for the analysis of traffic flows (Wen et al. 2017; Carmody and Sowers 2021), to the best of our knowledge, our work is the first to leverage insights and tools from braid theory, contributing a new perspective that ties symbolic and quantitative perspectives on understanding the complexity of traffic flows. The tools discussed in this paper, and especially the Topological Complexity index (Dynnikov and Wiest 2007) (Sec. 4.1) may augment existing methods for

scenario generation (Li et al. 2023; Fontaine and Nikolaidis 2022) and for assessing the interactivity of multiagent interactions (Tolstaya et al. 2021).

2.3. Topological representations in robotics

Robotics research has interfaced substantially with the field of topology as topological representations and tools offer great rigor, expressiveness, and interpretability. Notable examples where topological perspectives found successful applicability include the study of configuration spaces (Ghrist 2001), motion planning (Koditschek and Rimon 1990), and grasping (Rodriguez et al. 2012). Recently, there is an increasing interest manifested in numerous robotics applications such as untangling (Grannen et al. 2021), knitting (Lin and McCann 2021), knot planning (Yan et al. 2020), aircraft conflict resolution (Hu et al. 2000), multiagent navigation (Diaz-Mercado and Egerstedt 2017; Xiaolong Wang, 2022), and filtering (Tovar et al. 2014) as well as in dedicated workshops (Jaquier et al. 2021). These works often leverage technical tools drawn from homotopy theory (Cao et al. 2019; Bhattacharya and Ghrist 2018), persistent homology (Pokorny et al. 2016), fiber bundles (Orthey et al. 2020), and low-dimensional topology (Mavrogiannis and Knepper 2019; Yan et al. 2020) among others. In particular, in prior work, we have made use of topological abstractions such as invariants (Mavrogiannis et al. 2022b; Mavrogiannis and Knepper 2021; Roh et al. 2020; Berger 2001) and braids (Ghrist 2001; Mavrogiannis et al. 2017; Mavrogiannis and Knepper 2019) as multiagent motion primitives for navigation domains. Following up on some of our earlier work, braids have been emerging as a promising abstraction paradigm for complex multiagent interactions across several domains, such as autonomous driving (Wang et al. 2022a) and planning for tethered drones (Cao et al., 2023a, 2023).

In this paper, we are following up on this latter body of work by employing topological braids (Thiffeault 2022) as an abstraction of multiagent traffic behavior. In our past work, we used braids as symbolic primitives of multiagent collision avoidance in crowd navigation tasks (Mavrogiannis et al. 2017; Mavrogiannis and Knepper 2019). In those domains, we showed that a braided representation of multiagent behavior may enable a group of non-communicating agents to coordinate efficient collision-avoidance strategies in a distributed fashion. However, our approach lacked a way of handling obstacles and was only tested in open-space domains. In this paper, we expand the use of braids to constrained domains like urban road scenes. We first describe a mapping of traffic trajectories to a modified braided representation (Mavrogiannis and Knepper 2019). We then demonstrate how this representation may cluster different types of multiagent interactions in real-world traffic and assist in understanding the intrinsic complexity of road scenes. Finally, we introduce a probabilistic inference mechanism that predicts braids of multiagent interaction given observation of agents' past behaviors in a road scene. This mechanism handles the geometric structure of a road scene through the discretization of multiagent behavior into a set of multiagent paths.

2.4. Multiagent coordination in driving domains

In parallel, there has been rich interest in algorithmic approaches for multiagent coordination in driving domains. For example, Zanardi et al. (2022) propose a game-theoretic framework that incorporates reasoning about ranked individual drivers' preferences and communal welfare objectives. Sadigh et al. (2018) plan intent-expressive maneuvers that reinforce safe and efficient coordination in mixed traffic scenarios, whereas Lazar et al. (2018) plan optimal lane changes that reinforce prosocial behaviors such as platooning to increase capacity in congested highways. Lindemann et al. (2022) provide safety guarantees at intersection crossing scenarios leveraging conformal prediction as a tool for uncertainty quantification over trajectory estimates.

Some works focus on centrally managed intersections. Buckman et al. (2019) plan vehicle rearrangements using a social psychology metric to reduce system delays in centrally managed intersections, whereas Miculescu and Karaman (2019) develop a centralized control framework with safety and efficiency guarantees for continuous car flows at an unsignalized intersection. Bozga and Sifakis (2022) recover a safe centralized multiagent control policy that abides by a set of traffic rules formulated in the form of linear temporal logic specifications.

Many works apply tools from belief-space planning to the problem of safe lane merging (Bandyopadhyay et al. 2013; Sezer et al. 2015; Bouton et al. 2017; Hubmann et al. 2017; Hsu et al. 2018), whereas Pierson et al. (2018) propose a congestion cost function that enables agents to plan lane changes within desired risk levels. Some approaches focus on dealing with occlusions and faulty perception using probabilistic modeling (McGill et al. 2019) or deep reinforcement learning (Isele et al. 2018). Finally, relevant to our work is the approach of Patwardhan et al. (2023) who develop an optimization framework that leverages local message passing among vehicles to extract safe and efficient multiagent motion plans.

In this work, we demonstrate the value of the representation of topological braids for coordinating complex traffic scenarios like crossing an uncontrolled intersection. Unlike much of the literature, we focus on a setup that involves no explicit communication or a priori collision-avoidance protocols among agents: agents base their decision-making solely on the observation of the kinematic states of each other. Specifically, we describe a probabilistic inference mechanism that predicts braids of future multiagent behavior given observations of agents' state history. Based on this inference, we describe a decision-making scheme that

generates uncertainty-reducing actions. This scheme enables non-communicating agents with noisy behavior models of each other to coordinate safe and efficient traversals of uncontrolled intersections. Through extensive simulations, we demonstrate the scaleability of our approach to multiple scenarios involving agents with different behavioral models.

3. Abstracting road traffic into a topological braid

We introduce a representation based on topological braids (Artin 1947) that captures critical interaction events in road environments (e.g., overtaking, merging, crossing). This representation describes such interactions as sequences of symbols describing topological relationships between agents; any possible interaction manifests as a unique symbolic description of their trajectories. In the following subsections, we frame the notion of interaction in road traffic based on the literature, and then adapt our earlier braided representation (Mavrogiannis and Knepper 2019) to capture multiagent interactions in road environments.

3.1. Social interactions in road traffic

One of the most challenging problems in the space of autonomous vehicles is the modeling of behavioral dynamics among different actors in road environments. The inherent unobservability of agents' internal states, the inter-agent variability, local customs, and the dynamic context—among other factors—may give rise to multiagent social interactions that are hard to model. Wang et al. (2022a) define social interaction in road traffic as:

> **Definition 1.** (Social interaction in road traffic). A dynamic sequence of acts that mutually consider the actions and reactions of individuals through an information exchange process between two or more agents to maximize benefits and minimize costs.

This definition emphasizes the structure of the mechanisms that shapes agents' decision-making in road environments. Such mechanisms govern human–human, robot-human, or robot–robot encounters and allow for the response to real-world nuances including social norms and violation of traffic rules. While there are different ways to model or reproduce such mechanisms (e.g., game theory (Zanardi et al. 2022), formal methods (DeCastro et al. 2020), decision theory (Bouton et al. 2017)), in this work, we focus on the applicability of tools from low-dimensional topology. These tools provide a global abstraction of multiagent interaction in an interpretable, symbolic form that is useful for both analysis and the development of online approaches for prediction and control.

3.2. Domain

Consider a structured domain $\mathcal{Q}\subseteq\mathbb{R}^2$, where $n > 1$ agents are navigating from time $t = 0$ to a finite final time t_∞. $q_i \in \mathcal{Q}$ defines the position of agent $i \in \mathcal{N} = \{1, \ldots, n\}$ with respect to a fixed reference frame. Agent i follows a trajectory $\xi_i : [0, t_\infty] \to \mathcal{Q}$. Collectively, agents follow a system trajectory $\Xi = (\xi_1, \ldots, \xi_n)$. This trajectory is a detailed representation of the collective strategy that agents followed to avoid each other while following their paths. Their strategy can be summarized as a set of discrete relationships, such as the passing sides or crossing order of agents. These relationships are formed as a result of the geometric structure of the environment, traffic regulations, and agents' policies. In this paper, we show that such relationships feature topological properties that can be succinctly captured by the representation of topological braids (Artin 1947).

3.3. Topological braids

A braid is a tuple $b_f = (f_1, \ldots, f_n)$ of functions $f_i : I \to \mathbb{R}^2 \times I$, $i \in \mathcal{N}$ defined on a domain $I = [0, 1]$ and embedded in an Euclidean space $(\hat{x}, \hat{y}, \hat{t})$. These functions, called *strands*, are monotonically increasing along the $\hat{t}$ direction, satisfying the properties: (a) $f_i(0) = (i, 0, 0)$ and $f_i(1) = (p_f(i), 0, 1)$, where $p_f : \mathcal{N} \to \mathcal{N}$ is a permutation in the symmetric group N_n and (b) $f_i(t) \neq f_j(t)\ \forall\ t \in I, j \neq i \in \mathcal{N}$. Two braids, $b_f = (f_1, \ldots, f_n)$, $b_g = (g_1, \ldots, g_n)$, can be composed through a *composition* operation (Figure 2): their composition, $b_h = b_f \cdot b_g$, is also a braid $b_h = (h_1, \ldots, h_n)$, comprising a set of n curves, defined by Murasugi and Kurpita (1999) as

$$h_i(t) = \begin{cases} f_i(2t), & t \in \left[0, \frac{1}{2}\right), \\ g_j(2t-1), & t \in \left[\frac{1}{2}, 1\right], \end{cases} \tag{1}$$

where $j = p_f(i)$. The set of all braids on n strands, along swith the composition operation form a group, B_n, called the Braid group on n strands. Following Artin's presentation (Artin 1947), the braid group B_n can be generated from $n - 1$ primitive braids $\sigma_1, \ldots, \sigma_{n-1}$ (see Figure 1), called generators, and their inverses, via composition.

A **generator** is a braid $\sigma_i = (\sigma_1, \ldots, \sigma_n)$, $i \in \mathcal{N}\backslash\{n\}$ for which: (a) $\sigma_i(0) = (1, 0, 0)$, and $\sigma_i(1) = (p_i(i), 0, 1)$, where $p_i : \mathcal{N} \to \mathcal{N}$ is an adjacent transposition swapping i and $i + 1$; (b) there exists a unique $t_c \in [0, 1]$ such that $(\sigma_i(t_c) - \sigma_{i+1}(t_c)) \cdot \hat{x} = 0$ and $(\sigma_i(t_c) - \sigma_{i+1}(t_c)) \cdot \hat{y} > 0$.

The **inverse** of σ_i is the braid $\sigma_i^{-1} = (\sigma_1^{-1}, \ldots, \sigma_n^{-1})$, $i \in \mathcal{N}\backslash n$, for which: (a) $\sigma_i^{-1}(0) = (1, 0, 0)$ and $\sigma_i^{-1}(1) = (p_i(i), 0, 1)$; (b) there exists a unique $t_c \in [0, 1]$ such that $(\sigma_i^{-1}(t_c) - \sigma_{i+1}^{-1}(t_c)) \cdot \hat{x} = 0$ and $(\sigma_i^{-1}(t_c) - \sigma_{i+1}^{-1}(t_c)) \cdot \hat{y} < 0$.

The **identity** braid $\sigma_0 = (\sigma_1^0, \ldots, \sigma_n^0)$ implements no swap, that is, $p_0(k) = k$ for any $k \in \mathcal{N}\backslash\{n\}$, yielding

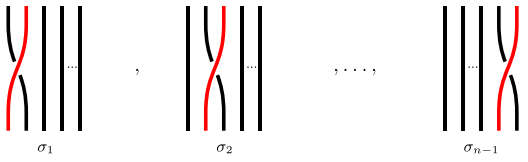

Figure 1. Presentation of the braid group, B_n. The group can be generated by the $n-1$ elements shown above, called generators (and their inverses), using an operation called composition (see Figure 2).

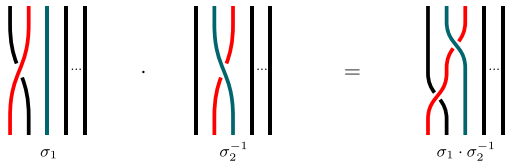

Figure 2. Composition of braids. Algebraically, the composition of two braids is represented as a product. Geometrically, this operation involves stacking of the braids on top of each other as shown.

$\sigma_k^0(0) = (k, 0, 0)$, $\sigma_k^0(1) = (k, 0, 1)$ and it holds that $\nexists t_c \in [0, 1]$ such that $(\sigma_k^0(t_c) - \sigma_{k+1}^0(t_c)) \cdot \hat{x} = 0$.

Any braid can be written as a *word*, that is, a product of generators and their inverses (Figure 2), satisfying the *relations*

$$\begin{aligned} \sigma_i\sigma_j &= \sigma_j\sigma_i, |j-i| > 1, \\ \sigma_i\sigma_{i+1}\sigma_i &= \sigma_{i+1}\sigma_i\sigma_{i+1}, \forall i. \end{aligned} \tag{2}$$

3.4. Transforming traffic trajectories into braids

We will convert a system trajectory Ξ into a geometric object with the structure of a topological braid through a sequence of operations that retain the topological relationships among agents' trajectories in Ξ.

We define by $\xi_i^x : [0, t_\infty] \to \mathbb{R}$ and $\xi_i^y : [0, t_\infty] \to \mathbb{R}$ the x and y projections of ξ_i. For $t = 0$, ranking agents in order of increasing $\xi_i^x(0)$, $i \in \mathcal{N}$ value defines a starting permutation $p_s : \mathcal{N} \to \mathcal{N}$, where $p_s(i)$ denotes the order of agent i. For $t = t_\infty$, ranking agents in order of increasing $\xi_i^x(t_\infty)$ value defines a final permutation $p_d : \mathcal{N} \to \mathcal{N}$, where $p_d(p_s(i))$ denotes the final ranking of agent i. Thus, the execution in Ξ can be abstracted into a transition from p_s to p_d.

We denote by τ: $I \to [0, t_\infty]$ a time normalization function, uniformly mapping $I = [0, 1]$ to the execution time in the range $[0, t_\infty]$. We then define the trajectory bounds as $x_{min} = \min_{i,t} \xi_i^x(t)$, $x_{max} = \max_{i,t} \xi_i^x(t)$, $y_{min} = \min_{i,t} \xi_i^y(t)$, and $y_{max} = \max_{i,t} \xi_i^y(t)$. Assuming $x_{max} \neq x_{min}$ and $y_{max} \neq y_{min}$, we define the ratio functions as

$$r_i^x(t) = \frac{\xi_i^x(t) - x_{min}}{x_{max} - x_{min}}, r_i^y(t) = \frac{\xi_i^y(t) - y_{min}}{y_{max} - y_{min}}. \tag{3}$$

Finally, we define a set of functions $(f_1, \ldots, f_n)$, with $f_j : I \to \mathbb{R}^2 \times I$, $j \in \mathcal{N}$, such that

$$f_j(a) = \begin{cases} (j, 0, 0), & a = 0 \\ \left(f_j^x(a), f_j^y(a), a\right), & a \in (0, 1) \\ (p_d(j), 0, 1), & a = 1 \end{cases} \tag{4}$$

where

$$\begin{aligned} f_j^x &= 1 + r_j^x(\tau(a))(n-1), \\ f_j^y &= -1 + 2r_j^y(\tau(a)), \end{aligned} \tag{5}$$

and $j = p_s(i)$, $i \in \mathcal{N}$. For $a \in (0, 1)$, the expressions of (4) scale x-coordinates lie within $[1, n-1]$ and the y-coordinates lie within $[-1, 1]$ in a way that preserves topological relationships among trajectories. The set of functions $(f_1, \ldots, f_n)$ is a topological *braid* β following the definition of Section 3.3. The braid β is topologically equivalent (ambient-isotopic) to the system trajectory Ξ.

3.5. Braids as modes of traffic coordination

The transformation of Section 3.4 enables summarization of a traffic episode into a braid capturing multiagent collision-avoidance relationships. This braid can be written as a word, similarly to how Thiffeault (2010) converted particle motion in a fluid to a braid (Figure 3): a) we label any trajectory crossings that emerge within the x-t projection as braid generators by identifying *under* or over crossings (Figure 3(b)); b) we arrange these generators in temporal order into a *braid word*.

In Figure 3, four agents cross an intersection. The braid $\sigma_3\sigma_1\sigma_2^{-1}\sigma_3^{-1}\sigma_1^{-1} \in B_4$ is a description of how agents coordinated to avoid each other. The group B_4 contains all ways in which these four agents could possibly avoid each other. In a scene with n agents, a braid represents a *mode* of coordination from the set of possible modes in B_n.

Remark 1. *Note that alternative reference frames can be employed; we selected the $\hat{x}$-$\hat{t}$ plane projection for convenience. As discussed by Thiffeault (2010) and Boyland (1994), change in the projection plane generally changes a braid by conjugation. Two braids $\beta_1, \beta_2 \in B_n$ are conjugate if there exists a braid $g \in B_n$ such that $g^{-1} \cdot \beta_1 \cdot g = \beta_2$. In other words, the change of projection plane results in braids that are topologically equivalent and recoverable from one another. Thus, the choice of a projection plane does not alter the insights about traffic behavior; as long as the analysis is consistently using and reporting the projection plane (and thus the transform required to transition between different projections), any insights are reproducible. For convenience and consistency, we will maintain this convention throughout the paper. Thus, any insights from the topological analysis of real-world traffic in Section 4 are naturally relatable to simulated study of Section 6.*

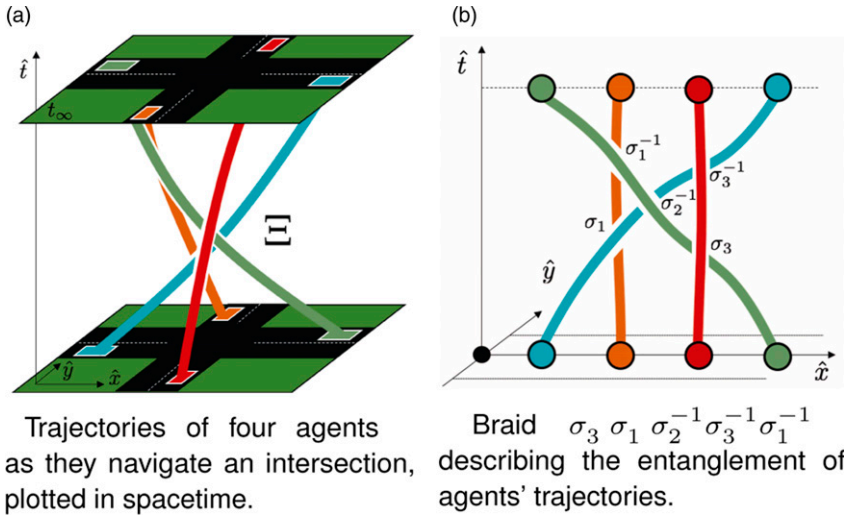

Figure 3. Transition from Cartesian trajectories (a) to topological braids (b) via equation (4) assuming a *x*-*t* projection.

3.6. Computational properties

To highlight the possible computational benefits arising from the summarization of traffic episodes into braids, we study the runtime of enumerating modes of coordination as topological braids in comparison to enumerating trajectories across space and time. Consider a traffic episode of H timesteps, involving n agents. Each agent has $\mathcal{T}$ options of routes to follow and $\mathcal{U}$ actions to take at every timestep. We assume that there is at most one agent per lane, that is, $n \leq \mathcal{T}$. The horizon of the execution is long and thus $n \ll H$. Further, $\mathcal{U}$ is a realistically rich space of controls and thus $n \ll \mathcal{U}$, $H \ll \mathcal{U}$, and $\mathcal{T} \ll \mathcal{U}$. Finally, we assume that agents are goal-driven for the horizon of each episode, and thus they will cross paths with each other at most once.

The number of possible spacetime trajectories in this domain is $N_c = |\mathcal{T}|^n(|\mathcal{U}|^n)^H$. Enumerating these trajectories runs in time $O(2^{nH\log\mathcal{U}})$. For the same scene, the number of possible braids generally depends on the structure of the road network. However, we can bound the number of possible outcomes as $N_b \geq 3^{\binom{n}{2}}$, where the exponent is the binomial coefficient representing the number of all pairs of agents, and the base represents the 3 types of possible interactions per pair that could be represented by a braid, that is, "over-crossing," "under-crossing," or no crossing. This enumeration runs in time $O(2^{n^2})$.

Theorem 1. The runtime of enumerating braids is lower than the runtime of enumerating trajectories in spacetime for the class of driving problems considered above.

We want to show that $2^{n^2} < 2^{nH\log\mathcal{U}}$. This inequality is equivalent to $n < H\log\mathcal{U}$. We assumed that $n \ll H$, $n \ll \mathcal{U}$, therefore, it should also hold that $n \ll H\log\mathcal{U}$. Thus, the initial inequality holds and supports the statement that the runtime of enumerating braids is significantly lower than the runtime of enumerating spacetime trajectories.■

4. Topological analysis of road traffic

In this section, we discuss a measure of topological complexity, developed on top of the braid formalism and demonstrate how it can be used to assess the interactivity of real-world road traffic.

4.1. Complexity of braid entanglement

The entanglement of the trajectories described by a braid is indicative of the complexity of the interaction between agents. We quantify braid complexity using the *Topological Complexity* index (TC) of Dynnikov and Wiest (2007) for which we provide an informal definition below.

Assume that a braid $\beta \in B_n$ represents the collective motion of n agents from initial locations $\beta(0)$ to final locations $\beta(1)$. Denote by D^2 a closed disk surrounding agents' initial positions, $\beta(0)$. Define by E a set of $n-1$ disjoint arcs, anchored on the disk, that separate the agents' positions at time $t = 0$. These arcs define n distinct regions in the disk. (see Figure 4). Assume that these regions are rigidly attached on the agents. As the agents follow the motion described by β from $t = 0$ to $t = 1$, the regions dynamically deform. The image $D = \beta \cdot E$ (i.e., the union of arcs obtained from E by the action of the braid β) representing the shape of the regions obtained upon applying the motion described by β on E is called a *curve diagram*. The *norm* of curve diagram D is defined as the number of intersections of D with the x axis. Based on the above definitions, we can define the TC index of a braid $\beta \in B_n$ as

$$TC(\beta) = \log_2(\|\beta \cdot E\|) - \log_2(\|E\|) \quad (6)$$

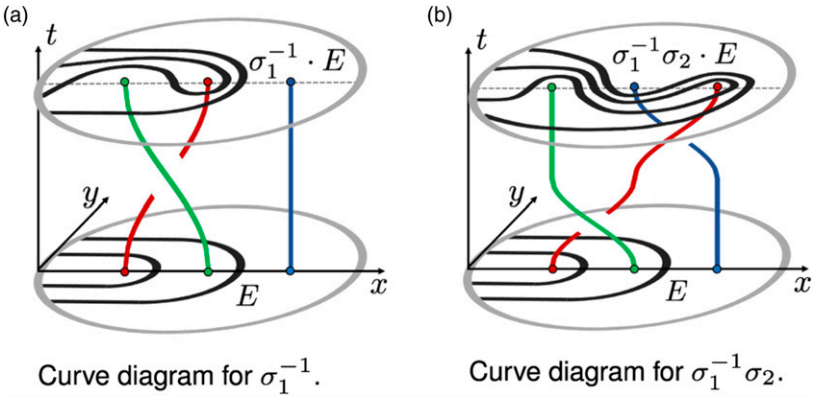

Figure 4. Curve diagrams for braids of different complexity. The braid $\sigma_1^{-1}\sigma_2$ (b) is more complex ($TC = 2$) than the braid σ_1^{-1} ($TC = 1.585$) shown in (a). Qualitatively, this can be traced in the higher number of intersections between the curve diagram $\sigma_1^{-1}\sigma_2 \cdot E$ and the x-axis (dotted line).

This expression is equivalent to the logarithm of the *gain* of intersections with the x-axis, upon application of a braid. Figure 4 depicts curve diagrams acquired upon inducing motion of two different braids on the canonical curve diagram E.

4.2. Application on real-world traffic datasets

We examine the inD (Bock et al. 2020), uniD (Bock et al. 2021), and rounD (Krajewski et al. 2020) datasets, containing trajectory data (of vehicles, pedestrians, and bicycles) recorded, respectively, in four intersection scenes and four roundabout scenes of the German road network. Both datasets were extracted from drone footage in 25fps via computer vision techniques, yielding an estimated positional error in the order of 10 cm. A top view of the eight scenes is shown in Figure 5, and their approximate dimensions are listed in Table 1. An example of how we transition from vehicle trajectories to topological braids in the inD (Bock et al. 2020) is shown in Figure 6.

4.2.1. Methodology. We split each scene into a set of sequential episodes, sweeping the whole duration of the recording. Each episode has a fixed duration of $\Delta T = 10$ s, containing trajectories of simultaneously navigating agents. From qualitative inspection, we observed that the most interesting interactions across all scenes involved vehicle traffic; to highlight dynamic vehicle traffic, we filtered out agents moving with low speeds below $v_{\min}$ and agents that are further than a threshold $d_{\min}$ from each other throughout the episode. Table 2 lists the exact thresholds used for our computations. The filtering process resulted in a set of episodes summarized in Table 1. For each scene, we note the number of episodes and the number of vehicles per episode. Using the framework of Section 3.3, we abstracted the trajectory of each episode into a compact braid, leveraging the braid relations of equation (2). Table 1 lists the number of unique braids per scene, the statistics of braid lengths per scene, and the statistics of TC per scene. The braid lengths correspond to the number of generators (crossings) of a braid. While the braid length is not a definitive measure for interaction complexity, (see Figure 4), it provides an intuitive idea of the type of interactions among agents: we see that braid length is positively correlated with the TC index. TC formalizes this intuition into a score which more clearly demonstrates the complexity of the interaction, as discussed in Section 4.1. We performed all computations using the Braidlab package (Thiffeault and Budisic 2013–2021).

> **Remark 2.** Note that the parameters of Table 2 were used to split the dataset into episodes and allow for a demonstration of our methodology. Depending on the goals of the analysis and the domain in consideration, different values could be selected to split a dataset into episodes.

4.2.2. Analysis. The behavior in each scene is clustered into a small number of unique braids, describing vehicles' interaction patterns (see Table 1). This highlights that real-world traffic tends to collapse to a small set of outcomes. The extracted braids are mapped onto the TC values on the right. We observe that on average the rounD scenes appear to contain more complex vehicle interactions as reflected in the increased TC values compared to the inD/uniD scenes. Figure 7 depicts episodes of varying TC, drawn from the two datasets, along with their braid representatives and TC scores. We see that complex interactions get mapped onto higher TC values.

Figure 8 shows the empirical cumulative density of TC across the inD and rounD dataset scenes. Note that a more linear density generally indicates greater diversity over the range of TC values, whereas stepwise-like patterns indicate lower diversity. We see that each scene has a distinct complexity growth pattern, but in both datasets, about 60% of episodes are concentrated below $TC = 1.5$. This is highlighted in Figure 9, which shows the relative frequency of unique braids per scene, organized in order of increasing TC. We see that the mass of the frequency is concentrated on

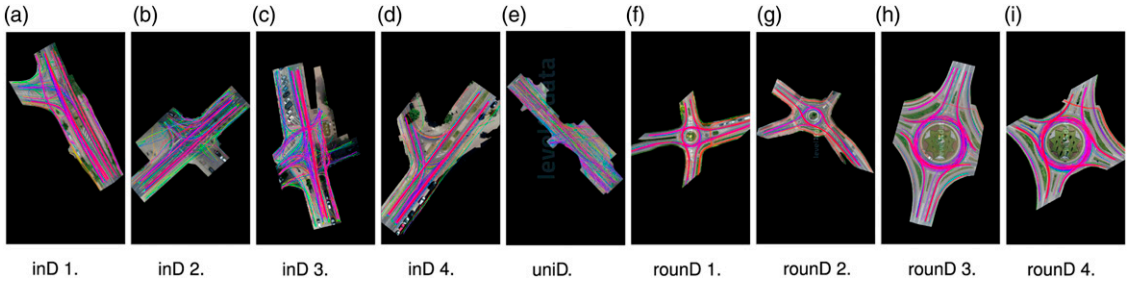

Figure 5. Top view of the 9 scenes from the inD (Bock et al. 2020), rounD (Krajewski et al. 2020), and uniD (Bock et al. 2021) datasets that we analyzed using topological tools. All trajectories are overlayed on top of the street structures.

Table 1. Scene Details and Interaction Statistics.

Scene	Dimensions (m^2)	Episodes	Vehicles/Episode (M, SD)	Unique braids	Braid length (M, SE)	TC (M, SE)
inD 1	131 × 110	347	3.62 ± 1.76	155	4.53 ± 0.29	1.62 ± 0.03
inD 2	59 × 64	254	2.82 ± 1.00	62	2.38 ± 0.15	1.48 ± 0.03
inD 3	85 × 45	386	2.62 ± 0.90	41	1.61 ± 0.08	1.28 ± 0.03
inD 4	79 × 67	174	4.10 ± 1.51	99	5.60 ± 0.34	1.79 ± 0.02
uniD	90 × 87	413	3.37 ± 1.49	117	2.88 ± 0.14	1.46 ± 0.02
rounD 1	99 × 143	58	3.16 ± 1.45	30	2.87 ± 0.48	1.20 ± 0.11
rounD 2	99 × 122	59	3.85 ± 1.75	32	4.01 ± 0.58	1.54 ± 0.06
rounD 3	127 × 69	574	4.36 ± 2.28	290	5.01 ± 0.26	1.43 ± 0.03
rounD 4	92 × 98	1050	4.07 ± 2.00	476	5.47 ± 0.21	1.46 ± 0.02

(a) inD 1, $TC = 0$. (b) inD 1, $TC = 1.5850$. (c) inD 1, $TC = 3.0444$. (d) inD 3, $TC = 0$. (e) inD 3, $TC = 1.5850$. (f) inD 3, $TC = 2.5850$. (g) rounD 1, $TC = 0$. (h) rounD 1, $TC = 1.4150$. (i) rounD 1, $TC = 2.9069$. (j) rounD 2, $TC = 0$. (k) rounD 2, $TC = 1.7162$. (l) rounD 2, $TC = 2.9386$. (m) rounD 3, $TC = 0$. (n) rounD 3, $TC = 1.2224$. (o) rounD 3, $TC = 3.2395$. (p) rounD 4, $TC = 0$. (q) rounD 4, $TC = 1$. (r) rounD 4, $TC = 3.3505$.

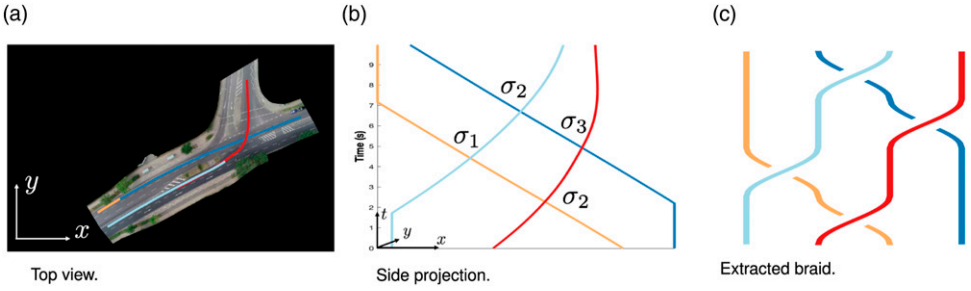

Figure 6. Transitioning from a real-world episode to a braid. The trajectories of (a) are first projected on the plane *x*-*t* (b) and then the braid $\sigma_2\sigma_1\sigma_3\sigma_2$ is reconstructed (c).

Table 2. Parameters of data analysis.

Parameter	Value	Description
ΔT	$10s$	Episode duration
$v_{\min}$	$14ms^{-1}$	Speed threshold
$d_{\min}$	$10m$	Distance threshold

the left side for both plots, suggesting that the majority of episodes feature a relatively low degree of interaction. This indicates that despite the dense traffic exhibited in the datasets (Table 1), the vast majority of episodes involve traffic that is orderly and well organized. This is an artifact of the underlying spatiotemporal structure (geometry, traffic rules, driving styles).

4.3. Discussion

Our representation enables enumeration of the classes of multiagent interaction patterns that are *theoretically* possible in a traffic scene in a compact and interpretable form. Further, given a traffic dataset, it allows us to extract the subset of interaction patterns that are *empirically* relevant. This may inform algorithmic design, benchmarking, and even road network design. Importantly, our framework can be valuable for characterizing a traffic dataset with respect to the support it provides over the space of theoretically possible behavior in a domain. Understanding the support of a dataset is crucial for data-driven approaches (Roh et al. 2020; Salzmann et al. 2020; Mavrogiannis et al. 2022a) but also for guiding the

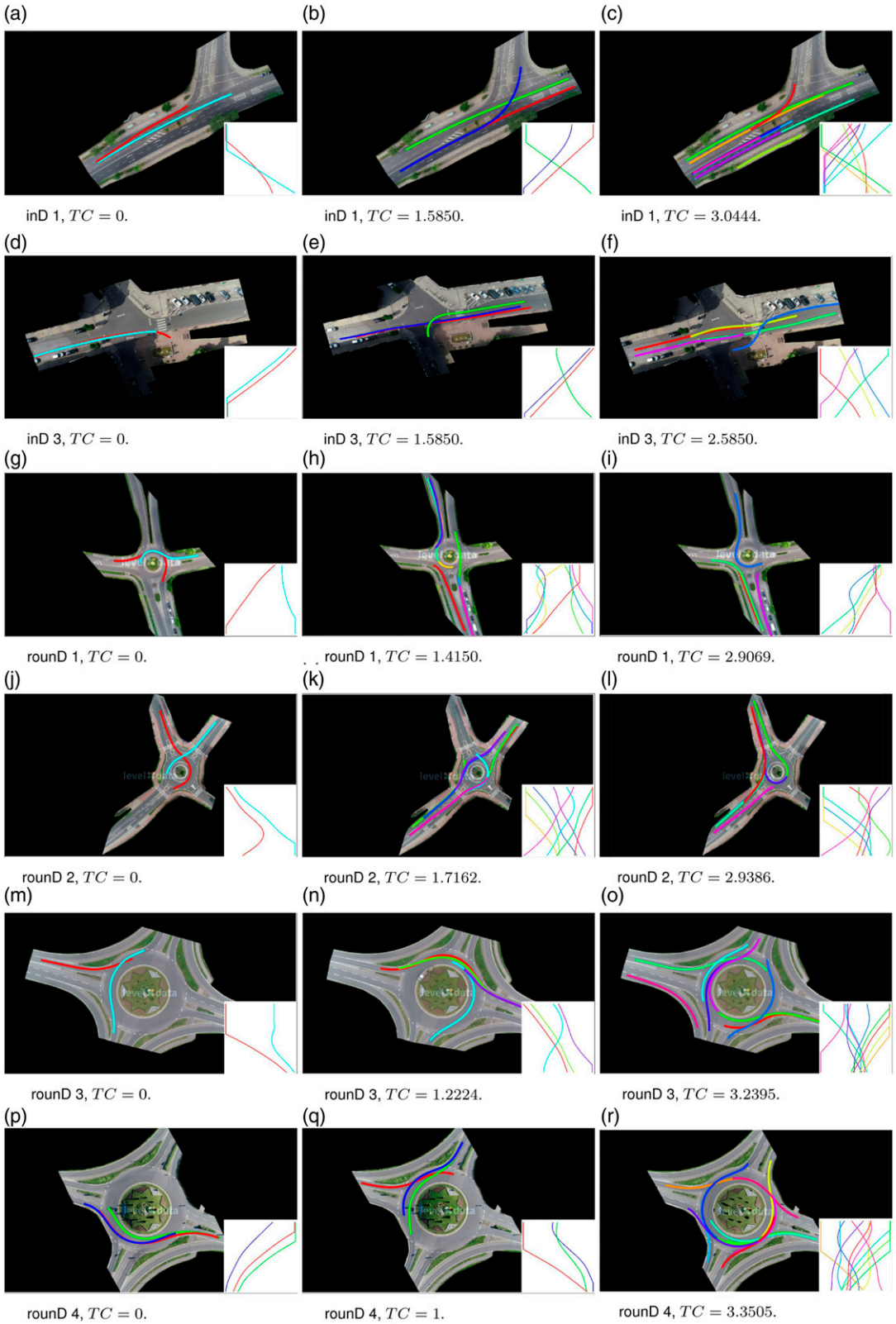

Figure 7. Episodes with different topological complexity (TC). Each row depicts three episodes yielding distinct braids in the same scene. At the bottom right of each figure, the braid formed by the data through an x-t side projection of the episode is plotted. The episodes on each row are organized from left to the right in order of increasing TC. In all scenes, the agents are following the right-hand traffic convention.

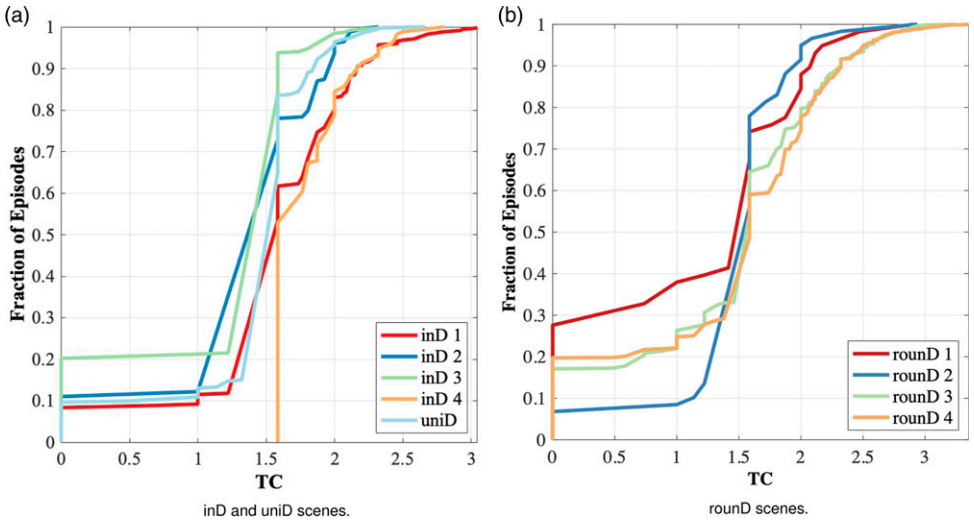

Figure 8. Cumulative density of TC (Topological Complexity index) in intersections (a) and roundabouts (b).

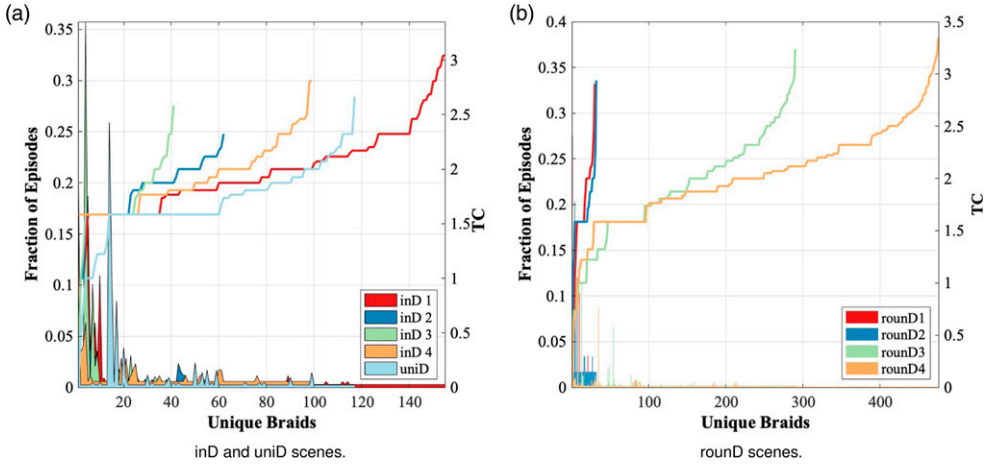

Figure 9. Frequency of unique braids in intersections (a) and roundabouts (b), arranged in order of increasing TC (Topological Complexity index).

process of synthetically generating simulated scenarios to produce diverse datasets.

Our framework is complementary to alternative approaches for characterizing interaction, such as the interactivity score (Tolstaya et al. 2021) and distribution-based KL-divergence. The interactivity score may miss crucial interaction events: scores can be large when there is high correlation between two trajectories (e.g., one car following another), but small when trajectories are dissimilar (e.g., cars crossing an intersection). In contrast, TC will account for these situations through the consideration of the underlying topological structure. Further, our framework may be directly applicable to any traffic dataset (Caesar et al., 2020; Chang et al., 2019; Ettinger et al., 2021) and even to alternative domains like pedestrian tracking (Pellegrini et al. 2009) or sports analysis (Alcorn and Nguyen 2021) without additional modifications. It may complement temporal logic approaches for trajectory labeling (Puranic et al. 2021; Li et al. 2021) which often require involved and domain-specific mathematical treatment (Schulz et al. 2017).

5. Reasoning about braids of road traffic

We describe a mathematical model that probabilistically maps past traffic behavior of agents to modes of future interactions among them (like who passed first/later, left/right), described in the form of topological braids. We discuss how this model can be used for online inference to facilitate decision-making in complex traffic scenes. For a concise reference of the key variables in our framework, the reader may refer to Table 3.

5.1. Problem statement

Consider the uncontrolled street intersection of Figure 12, where $n > 1$ non-communicating agents with car-like kinematics are

Table 3. Nomenclature.

Variable	Description
n	Number of agents
$\mathcal{N}$	Set of all agents, $\mathcal{N} = \{1, \ldots, n\}$
u_i	Control action of agent i (speed and steering angle)
$\mathcal{U}$	Space of controls, that is, $\mathcal{U} \subseteq \mathbb{R} \times \mathbb{S}$
U	Control profile, that is, set $U = \{u_1, \ldots, u_n\}$
τ_i	Path of agent i
T	System path, that is, $T = \{\tau_1, \ldots, \tau_n\}$
$\mathcal{T}$	Set of all possible system paths
T_i	Paths of all agents but i, that is, $T_i = \{t_j, j \in \mathcal{N} \backslash i\}$
ξ_i	Timed trajectory of agent i
Ξ	System trajectory, that is, $\Xi = \{\xi_1, \ldots, \xi_n\}$
Ξ'	Estimated future system trajectory
c	Boolean, indicating that Ξ contains collisions if true
β_i	Topology of trajectory Ξ from the perspective of agent i
$\tilde{\beta}_i$	Joint event that Ξ is equivalent to β_i and not in collision
B_n	Braid group, that is, set of all possible trajectory topologies

navigating. Denote by $q_i = (x_i, y_i, \theta_i) \in \mathcal{Q} \subseteq SE(2)$ the state of agent $i \in \mathcal{N} = \{1, \ldots, n\}$ with respect to (wrt) a fixed reference frame, defined by a basis $(\hat{x}, \hat{y}, \hat{t})$. Each agent i starts from an initial state $s_i \in \mathcal{Q}$, lying on a side of the intersection, and moves towards a final—unknown to others—state $d_i \in \mathcal{Q}$ lying on a different side. They do so by tracking a path $\tau_i : I \rightarrow \mathcal{Q}$, for which it holds that $\tau_i(0) = s_i$ and $\tau_i(1) = d_i$, where $I = [0, 1]$ is a path parametrization. Observing the complete system state $Q = (q_1, \ldots, q_n) \in \mathcal{Q}^n$, agent i tracks τ_i by executing a policy $\pi_i : \mathcal{Q} \rightarrow \mathcal{U}$, generating actions $u_i \in \mathcal{U}$ (speed and steering angle), where $\mathcal{U} \subseteq \mathbb{R} \times \mathbb{S}$ is a space of controls. Agent i is not aware of the intended path τ_j, the destination d_j, or the exact policy π_j of any other agent $j \neq i \in \mathcal{N}$, but is able to perfectly observe their state at every timestep.

We study the problem of designing a policy π_i that enables agents to fluently coordinate collision-free intersection crossings while following time-efficient trajectories under uncertainty in a distributed fashion and without explicitly communicating with each other. Note that trivial solutions like employing a first-come-first-served protocol requires a priori coordination; in this work, we are interested in the more challenging domain involving completely no coordination at all.

5.2. Decentralized navigation as braid prediction

We describe a probabilistic model that links past agents' trajectories to a braid representing the spatiotemporal entanglement of their future trajectories at an intersection domain. Figure 10 illustrates the setup of the proposed model in a four-agent scenario. Based on this mechanism, we build an optimization-based control scheme for decentralized navigation at uncontrolled intersections.

At time $t \in [0, t_\infty]$, agent i, having access to the complete system state history so far, that is, the set of all agents' trajectories $\Xi = \{\xi_1, \ldots, \xi_n\}$, maintains a belief $bel_i = P(\beta_i|\Xi)$ over the braid $\beta_i \in B_n$ that describes the topology of the emerging (future) system trajectory $\Xi' = \Xi_{t \rightarrow \infty}$ from the perspective of agent i. Note that each agent uses a distinct projection plane to define their own braid set. The braid β_i depends on agents' intended system path, that is, the set of all agents' intended paths $T = \{\tau_1, \ldots, \tau_n\}$. Agent i is unaware of the intended paths of others, $T_i = \{\tau_j, j \in \mathcal{N} \backslash i\}$ but maintains a belief over them, $P(T_i|\Xi)$. To capture this dependency, we marginalize over $\mathcal{T}_i$, the subset of all possible system paths from $\mathcal{T}$, for which agent i (the ego agent) follows its intended path

$$bel_i = P(\beta_i|\Xi) = \sum_{T_i \in \mathcal{T}_i} P(\beta_i|\Xi, T_i) P(T_i|\Xi). \tag{7}$$

For a given system path T, different braids could possibly emerge, depending on the path tracking behavior of agents. To capture this dependency, we marginalize the probability $P(\beta_i|\Xi, T_i)$ over the control profile $U \in \mathcal{U}^n$ that could be taken by agents at the current time step

$$P(\beta_i|\Xi, T_i) = \sum_{U \in \mathcal{U}^n} P(\beta_i|\Xi, U, T_i) P(U|\Xi, T_i). \tag{8}$$

Substituting in equation (7), we get

$$bel_i = \sum_{\mathcal{T}_i} \left\{ \sum_{\mathcal{U}^n} P(\beta_i|\Xi, U, T_i) P(U|\Xi, T_i) \right\} P(T_i|\Xi). \tag{9}$$

Equation (9) combines a local action selection model $P(U|\Xi, T_i)$ with a model of intent inference $P(T_i|\Xi)$ and a global behavior prediction model $P(\beta_i|\Xi, U, T_i)$.

The intention of agent $j \neq i$ over a path τ_j is conditionally independent of the intention of any other agent, given the past system trajectory Ξ. The probability over the path intention of agent j does not depend on the trajectories of others. Thus, we simplify the computation of the system path prediction as

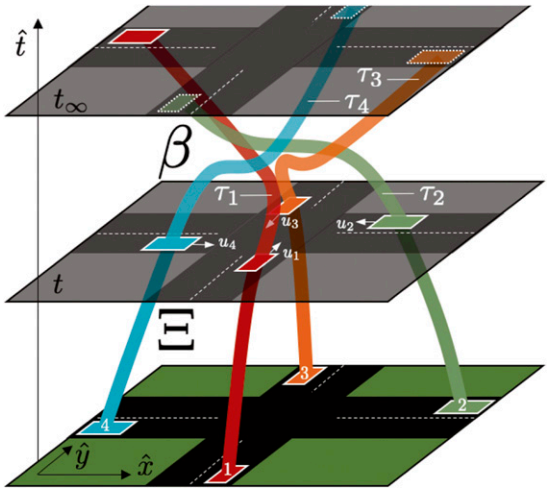

Figure 10. Topological inference. At time t, given state history Ξ, the ego agent (red), following path τ_1, predicts the topology β of the unfolding multiagent interaction.

$$P(T_i|\Xi) = \prod_{j \in \mathcal{N} \setminus i} P\left(\tau_j \middle| \xi_j\right), \tag{10}$$

where the product only considers the probabilities over the paths of others since agent i is certain about its own path.

Similarly, since agents select a control input independently, without having access to the policies of others, we decompose the computation of the control profile prediction as

$$P(U|\Xi, T_i) = \prod_{i=1}^{n} P(u_i|\Xi, T_i), \tag{11}$$

where the distribution $P(u_i|\Xi, T_i)$ represents the control input that agent i executes to make progress along its path τ_i, incorporating considerations such as preferred navigation velocity and a local tracking controller class.

The model of inference of equation (9) focuses on topology prediction, without considerations of collision avoidance. To filter out unsafe braids, we redefine equation (9) by incorporating a model of collision prediction. Define by c a boolean random variable representing the event that Ξ', the emerging future trajectory contains collisions (`true` for a collision, `false` for no-collision). $\tilde{\beta} = (\beta_i, \neg c)$ denotes the joint event that Ξ' is both topologically equivalent, that is, ambient-isotopic (Murasugi and Kurpita 1999) to a braid $\beta_i \in B_n$, *and* not in collision, that is, c is `false`. Then the belief, $\widetilde{bel}_i$, of agent i that $\tilde{\beta}_i$ is true can be computed as

$$\widetilde{bel}_i = P(\tilde{\beta}_i|\Xi)$$

$$= \sum_{\mathcal{T}_i} \left\{ \sum_{U} P(\tilde{\beta}_i|\Xi, U, T_i) P(U|\Xi, T_i) \right\} P(T_i|\Xi) \tag{12}$$

The occurrence of a collision is conditionally independent of the emerging braid—the braid only describes the topological pattern of the trajectories, ignoring any geometric intersections among the volumes of the vehicles. Thus, we may compute their joint distribution as

$$\begin{aligned} P(\tilde{\beta}_i|\Xi, U, T_i) &= P(\tilde{\beta}_i, \neg c|\Xi, U, T_i) \\ &= P(\neg c|\Xi, U, T_i) P(\beta_i|\Xi, U, T_i) \\ &= (1 - P(c|\Xi, U, T_i)) P(\beta_i|\Xi, U, T_i). \end{aligned} \tag{13}$$

5.3. Decision-making

An outcome $\tilde{\beta}_i$ represents a class of trajectories Ξ_{β_i} that are topologically equivalent to the braid β_i *and* not in collision. During execution, the distribution $P(\tilde{\beta}_i|\Xi, U, T)$ is reshaped as a result of agents' decisions. Our approach contributes towards a minimum-entropy shape of $P(\tilde{\beta}_i|\Xi, U, T)$, which corresponds to a state of consensus over a braid $\tilde{\beta}_i$ from the perspective of agent i. We do so through the following receding-horizon control scheme

$$u_i^* = \arg\min_{u_i \in \mathcal{U}} H(\tilde{\beta}_i), \tag{14}$$

where

$$H(\tilde{\beta}_i) = -\sum_{B_n} P(\tilde{\beta}_i|\Xi) \log P(\tilde{\beta}_i|\Xi), \tag{15}$$

is the information entropy of $P(\tilde{\beta}_i|\Xi)$, representing agent i's uncertainty over a solution $\tilde{\beta}_i$ where $P(\tilde{\beta}_i|\Xi)$ is recovered using equation (12). This optimization scheme contributes uncertainty-reducing actions over the emerging outcome $\tilde{\beta}_i$. Note that the use of the information entropy as a cost reflects the insight that multiple elements of B_n could be valid solutions to the collision-avoidance problem at a given instance. The ego agent behavior could still contribute to collision-free navigation even when there is not a unique winner within B_n, a strategy that has been successfully applied to domains like shared control (Javdani et al. 2018). An overview of our decision-making mechanism is depicted in Figure 11.

6. Distributed coordination at uncontrolled intersections via topological braids

We apply our decision-making mechanism in the task of navigating an uncontrolled intersection without relying on explicit communication among agents. Our goal is to understand the intrinsic value of reasoning about the topological structure of agents' collision-avoidance strategy compared to an approach of reasoning about trajectories in the Euclidean space.

6.1. Task

Our setup is the 4-way uncontrolled symmetric intersection of Figure 12. The dimensions of lanes as shown in Figure 12 are listed in Table 4. We assume that any side a is connected

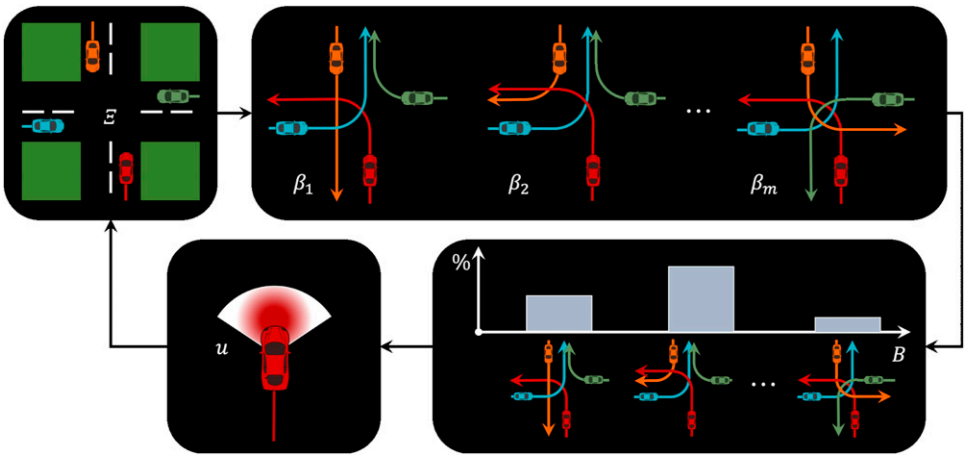

Figure 11. Decision-making scheme. At every cycle, the ego agent forward simulates a set of distinct futures, classifies them into topological outcomes, and selects the action that minimizes the uncertainty over such outcomes.

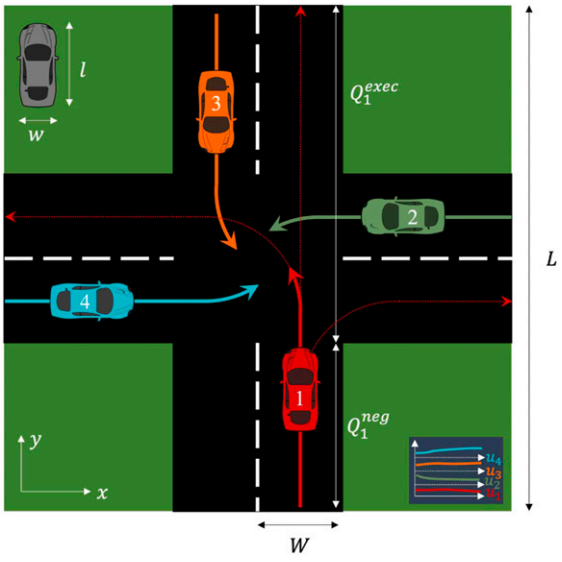

Figure 12. We study a minimalistic setup of decentralized navigation at uncontrolled intersections. By judiciously adjusting their speeds, agents during the negotiation phase (see speed graphs bottom right), agents may reach consensus over safe intersection traversals. We enable agents to represent possible strategies of traversal using the representation of topological braids.

Table 4. Parameters.

Parameter	Value	Description
L	$50m$	Lane length in (12)
W	$3.6m$	Lane width in (12)
l	$4.7m$	Car length in (12)
w	$1.7m$	Car width in (12)
a	10	Controls rate of change in (18)
δ	$15m$	Imminent collision threshold in (18)
$\mathcal{U}$	[5,10] (m/s)	Set of agents' preferred speeds

to any other side $b \neq a$ with a unique, publicly known legal path τ_{ab} lying along the middle of the lane. We assume that any agent $i \in \mathcal{N}$ that attempts to reach side b from side a will attempt to track this path, τ_{ab}.

Each agent follows a path out of three options, left, right, or straight, as shown in Figure 12 for agent 1. To avoid collisions with others, agent i considers $|\mathcal{T}_i| = 3^{n-1}$ possible system paths, extracted upon iterating over all possible combinations for other agents' paths. We consider a trial to be split into two phases: (a) the *negotiation* phase, which corresponds to the initial straight-path part of the intersection (denoted as $\mathcal{Q}_i^{neg}$ for agent i), within which the agent attempts to reach a consensus with others wrt a joint strategy of collision avoidance; (b) the *execution* phase, which corresponds to the rest of the path (denoted as $\mathcal{Q}_i^{exec}$ for agent i), within which the agent tracks the remainder of its path, by maintaining a constant speed. This design emphasizes the importance of proactive negotiation during the first portion and provides a natural metric of quality: the count of collisions during the execution part.

6.2. Models

Below, we describe models for the components of equation (15).

6.2.1. Decision-making. We assume that the process of decision-making described in (15) incorporates a PID controller internally that converts a speed v_i to a control input u_i, $i \in \mathcal{N}$. Thus, essentially agent i solves for an optimal speed v_i from a set $\mathcal{V}_i = \{v_i^{high}, v_i^{low}\}$, where v_i^{high} is a preferred high speed, and v_i^{low} is a low speed.

6.2.2. Intention prediction. We assume that agent i has no knowledge of the path τ_j of any other agent $j \neq i \in \mathcal{N}$, while j is in the negotiation stage. However, we assume that τ_j

becomes immediately obvious to agent i when agent j enters the intersection

$$P(\tau_j|\xi_j(t)) = P(\tau_j|q_j) = \begin{cases} \frac{1}{m} & \text{for } q_j \in Q_j^{neg} \\ 1 & \text{for } q_j \in Q_j^{exec}, \end{cases} \quad (16)$$

where $q_j = \xi_j(t)$ is agent j's current state, and $m = 3$ is the number of paths that agent j selects from.

6.2.3. Behavior prediction. Here, $P(u_j|\Xi, T)$ expresses the belief of agent i that agent $j \in \mathcal{N}$ will execute a control input u_j in the next timestep. Agent i knows that other agents employ the same PID controller and assumes that $\mathcal{V}_j = \mathcal{V}_i$. Agents generally prefer the high speed, which we encode in a distribution $P(v_j|\xi_j, \tau_j) = P(v_j)$. For each agent, $P(v_j = v_j^{high})$ is sampled at random from the range [0.6, 0.8] and remains fixed throughout the execution. Note that a speed v_j is deterministically mapped to a control input u_j through the low-level controller, thus $P(u_j|\xi_j, \tau_j) = P(v_j)$. Each agent i has a noisy estimate about the speed preferences of others: it assumes that others have the same exact preferences.

6.2.4. Topology prediction. To extract the probability of a topological outcome, agent i rolls out a system trajectory Ξ' for each path set $T \in \mathcal{T}_i$, considering all possible speed combinations from $\mathcal{V}^n$. Each rollout is then mapped to braid word β_i by projecting Ξ' onto a selected plane, as described in Section 3.4. For convenience and generality, each agent uses a distinct projection plane defined by a local x axis (see Figure 10) and the time axis. This process results in a set $B \subset B_n$ containing the set of all braids that could be realizable in the remainder of the execution. We model the probability that a future trajectory is equivalent to a braid $\beta^* \in B$ as follows

$$P(\beta_i = \beta^*|\Xi, U, T_i) = \frac{1}{z}\sum 1(\Xi', \beta^*), \quad (17)$$

where the indicator function $1(\Xi, \beta^*) = 1$ if a trajectory Ξ' is topologically equivalent to the braid $\beta*$ and 0 otherwise, and z is a normalizer across B. We perform the above computations using the Braidlab (Thiffeault and Budišić 2013–2021) package.

6.2.5. Collision prediction. During the rollouts detailed above, for each trajectory Ξ', we compute a minimum inter-agent distance d. We model the probability of a collision $P(c|\Xi, U, T_i)$ as follows

$$P(c|\Xi, U, T_i) = \frac{1}{1 + e^{a(d-\delta)}}, \quad (18)$$

where a controls the rate of change of the function, and δ denotes a threshold distance beyond which collision is imminent. According to this model, the smaller $d_{\min}$ is, it is exponentially more likely to have a collision.

6.2.6. Parameters. Table 4 lists environment and model parameters used in our evaluation.

6.3. Experimental setup

We describe our experimental setup involving the execution of a series of scenarios with our framework and a set of baselines.

6.3.1. Scenarios. We define a series of scenario classes, shown in Figure 13, designed to give rise to challenging multiagent interactions and help us characterize the robustness of our framework to different types of behavior. We designed these scenarios following some of the highest-severity scenarios defined in the *Pre-crash scenario typology for crash avoidance research* of the National Highway Transportation Safety Administration (Najm et al. 2007). While many of those scenarios involve only two agents, in our evaluation, we also explore the scalability of our system to scenarios involving up to four agents simultaneously. Note that our approach is applicable to scenarios with more agents; in this paper, we studied scenarios with up to four agents as an empirical upper bound in scenarios frequently encountered in uncontrolled intersections. Our scenarios are defined as follows:

Straight. All agents are moving straight in their respective lane, that is, each agent moves between the endpoints of a different lane. This scenario is equivalent to the *straight crossing paths at non-signalized junctions* scenario, defined by Najm et al. (2007). In our instantiation, we assume that all agents are running the same algorithm for inference and control.

Turn. This scenario is identical to *Straight* with the only difference that agent 1 is turning left instead of going straight. This scenario is equivalent to the *Vehicle(s) Turning at Non-Signalized Junctions*, defined by Najm et al. (2007).

Aggressive I. This scenario is identical to *Straight* with the only difference that agent 1 is *aggressive*, that is, it does not account for collision avoidance and navigates straight with maximum speed. This scenario is equivalent to the *running red light* and the *running stop sign* scenarios defined by Najm et al. (2007).

Aggressive II. This scenario is identical to *Aggressive I* with the only difference that agent 3 is also *aggressive*, that is, it does not account for collision avoidance and navigates straight with maximum speed.

6.3.2. Trials. To characterize the scalability of our framework, we define three instances of each scenario class, each corresponding to a different number $n \in \{2, 3, 4\}$ of navigating agents. To extract statistical insights, for each instance, we define a set of experimental trials by varying agents' speed preferences. For the *Straight* scenario, we generate 144 trials by drawing 12 evenly spaced speeds from $\mathcal{U}$ and assigning all possible combinations of them to the two agents. For the *Turn* scenario, we generate 125 trials by drawing 5 evenly spaced speeds from $\mathcal{U}$ and assigning all possible combinations of them to the three agents. For the

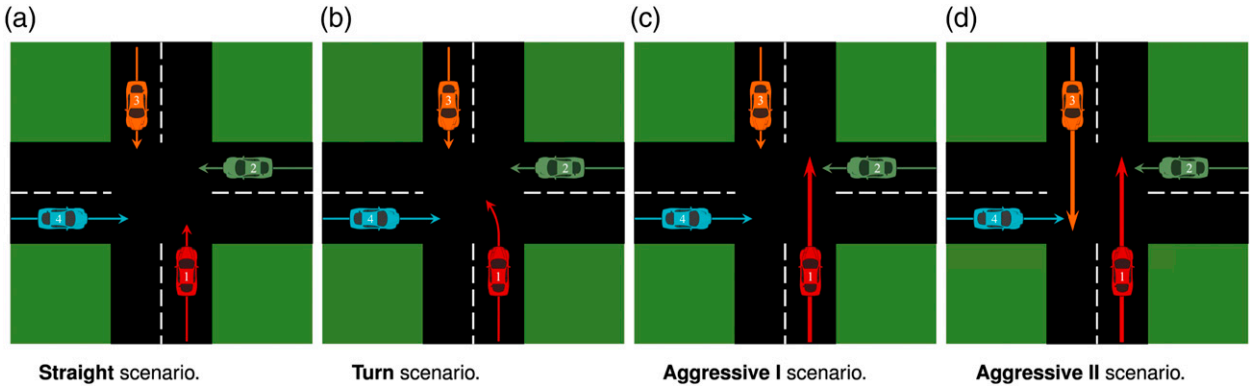

Figure 13. The four scenarios tested in our evaluation. In (a), all agents are heading straight. In (b), the red agent is turning left and the rest are heading straight. In (c), all agents are heading straight, but the red agent is moving straight without accounting for collision avoidance. In (d), all agents are heading straight, but the red and orange agents (1 and 3, respectively) are moving straight without accounting for collision avoidance.

Aggressive scenarios, we generate 81 trials by drawing 3 evenly spaced speeds from $\mathcal{U}$ and assigning all possible combinations of them to the three agents.

6.3.3. Conditions. We execute each set of trials and scenario class under 5 different conditions. Each condition corresponds to a different algorithm executed by agents:

Constant velocity. Agents track their desired paths with their desired speeds, without accounting for avoiding collisions with others. This condition serves as a reference of the intensity of interactions for each scenario.

Braids | unknown paths. Our complete proposed algorithm from equation (14).

Braids | known paths. A modification of our proposed algorithm that assumes knowledge of the paths that other agents are following, that is, they replace equation (12) with

$$\widetilde{bel}_i = \sum_U P(\tilde{\beta}_i|\Xi, U, T_i)P(U|\Xi, T_i). \tag{19}$$

No braids | unknown paths. A variation of *braids | unknown paths* that does not use braids for clustering trajectory sets. Specifically, agents reason about the emerging collision-free system trajectory $\tilde{\Xi}_i$ (instead of $\tilde{\beta}_i$), replacing equation (12) with

$$\widetilde{bel}_i = P(\tilde{\Xi}_i|\Xi, U, T_i)P(U|\Xi, T_i)P(T_i|\Xi). \tag{20}$$

No braids | known paths. A modification of *no braids | unknown paths* that assumes knowledge of the paths that others are following, that is, we replace equation (20) with

$$\widetilde{bel}_i = P(\tilde{\Xi}_i|\Xi, U, T_i)P(U|\Xi, T_i). \tag{21}$$

6.4. Results

Table 5 lists statistics of interaction among agents across simulated experiments. Figure 14 displays the collision frequency and the time to goal under the 5 conditions across the 3 scenarios classes considered. Figure 15 displays the time to goal performance for the collision-free trials. The performance of *constant velocity* acts as a reference, giving us an upper bound on collision frequency and a lower bound on time to destination, representing the hardness of the scenarios considered. Across conditions and scenarios, we generally see a trend of increased collision frequency and time to goal as the number of agents increases. In terms of collision frequency, we see that the braids-based approaches generally outperform the trajectory-based ones across scenarios with the performance gap becoming especially pronounced as the number of agents increases. In terms of time to destination, we generally see that braid-based approaches are slower overall, although not significantly so.

More specifically, in the *Straight* scenario (Figure 13(a)), compared to the trajectory-based baseline, *no braids | unknown paths*, our main algorithm, *braids | unknown paths*, reduces collision frequency by: 95% in 2-agent trials; 85% in 3-agent trials; and 66% in 4-agent trials (Figure 14(a)). We also see that knowledge of other agents' destinations helps the *braids | known paths* variant achieve even lower collision frequency, more evidently in the 4-agent trials. The price that the braid-based approaches pay is the increased time to destination (Figure 15(a)): they are on average about 4*s* slower across the 2-agent trials but this gap fades across the more complex ones with 3 and 4 agents.

In the *Turn* scenario, which represents a challenging instance of an *unprotected left* (Figure 13(b)), all algorithms are struggling beyond the 2-agent trials (Figure 14(b). This is because this scenario gives rise to more challenging encounter that may simultaneously involve all agents without any mechanism for explicit or a priori coordination. The braids-based approaches maintain their advantage compared to the trajectory-based baselines. Compared to *no braids | unknown paths*, our main algorithm, *braids | unknown paths*, is: 88% safer across 2-agent trials; 29% safer across 3-agent trials; and

Table 5. Topological Analysis of Simulated scenarios.

Scenario	Vehicles	Episodes	Unique braids	Braid length (M, SE)	TC (M, SE)
Straight	2	720	2	1.00 ± 0.00	1.58 ± 0.00
Turn	2	720	2	1.00 ± 0.00	1.58 ± 0.00
Aggressive I	2	720	2	1.00 ± 0.00	1.58 ± 0.00
Straight	3	625	4	2.00 ± 0.00	1.85 ± 0.00
Turn	3	625	14	2.69 ± 0.01	2.13 ± 0.01
Aggressive I	3	625	4	2.00 ± 0.00	1.88 ± 0.00
Aggressive II	3	625	4	2.00 ± 0.00	1.87 ± 0.00
Straight	4	405	42	5.00 ± 0.00	2.43 ± 0.02
Turn	4	405	113	5.70 ± 0.03	2.47 ± 0.02
Aggressive I	4	405	41	5.00 ± 0.00	2.48 ± 0.02
Aggressive II	4	405	37	5.00 ± 0.00	2.53 ± 0.02

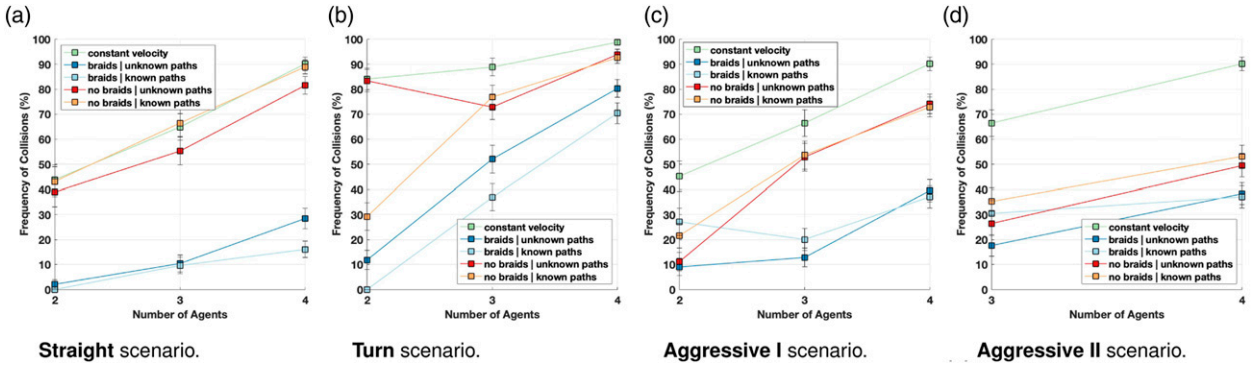

Figure 14. Collision frequency across trials per scenario. Error bars represent standard deviations.

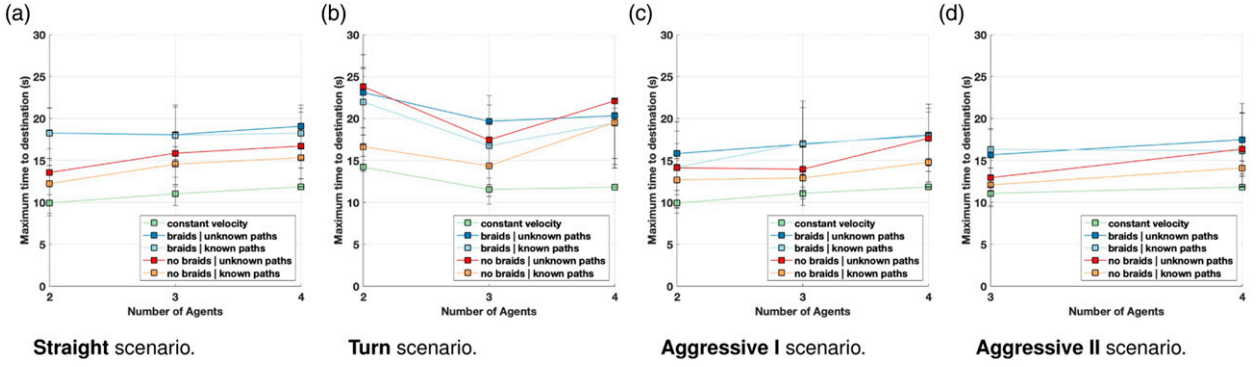

Figure 15. Maximum time to destination across collision-free trials per scenario. Each datapoint represents the average value over trials for the same number of agents. Error bars represent 25/75 percentiles.

13% safer across 4-agent trials. Knowledge of other agents' paths helps here as well, reducing collisions by about 10% across trials. In terms of time efficiency, rankings are more mixed; we still see braids-based approaches to take more time but not significantly so.

The *Aggressive I* scenario (Figure 13(c)) is challenging because agent 1 violates other agents' expectations about its behavior dynamics. Across algorithms, we see that agents can more effectively handle an aggressive agent compared to a reactive or a turning agent. This is because the aggressive agent is exhibiting more predictable behavior that agents can more easily anticipate. We also see that the *braids | unknown paths* algorithm handles this scenario well, with its collision frequency being visibly lower across 3- and 4-agent trials (75% and 45% reduction, respectively). Interestingly, we see that knowledge of agents' paths does not yield a visible advantage; being conservatively cautious rewards agents in the 2- and 3-agent scenarios as they can more robustly react to the unexpected decision-making of agent 1. In terms of time efficiency, we still observe the trend of braids-based approaches being slower but it is not significant.

In the *Aggressive II* scenario (Figure 13(d)), both agent 1 and agent 3 violate other agents' expectations about their behavior dynamics. Similarly to the *Aggressive I* scenario, we see that all algorithms adapt effectively to the predictable style of the aggressive agents and reduce their collision rates. Braids-based approaches maintain their lead, exhibiting significantly safer behavior for both 3- and 4-agent scenarios. In terms of time efficiency, we see comparable performance to the *Aggressive I* scenario across algorithms.

Finally, in Table 5, we see a topological analysis of the interactions observed among agents across simulated experiments. Each line lists statistics across all conditions per scenario. We generally see that increase in the number of agents leads to increase in the interaction complexity, manifested in longer braids and higher topological complexity. Additionally, we see that the *Turn* scenario yields highly diverse interactions, as shown in the increased number of unique braids. However, this diversity is not reflected in interaction complexity which remains similar to the other scenarios. It is worth noting that the simulated experiments conducted in this study exhibited higher topological complexity than the episodes observed in the traffic datasets examined in Section 4. This highlights the sparseness of interactions that are often captured in hours of traffic datasets but also the promise of carefully designed simulations for testing important components of autonomous-driving technology.

Each scenario is instantiated in three variants involving 2, 3, and 4 agents. The 2-agent variants involve agents 1 and 2; the 3-agent variants involve agents 1, 2, and 3; 4-agent variants involve agents 1 and 2, 3 and 4.

6.5. Discussion

Overall, we saw that the braids-based approaches exhibited superior performance across all scenario instances in terms of collision frequency. Although time efficiency was lower than baselines, the gap was not as significant across most scenarios.

6.5.1. Braids model domain structure. We attribute the performance gains of braids-based approaches to the incorporation of multiagent interaction modeling into agents' decision-making. The trajectory-based approaches we tested tend to ignore the structure of multiagent decision-making in this domain; while they reason about how other agents' destinations may affect their behavior, they fail to incorporate the structure of multiagent collision avoidance imposed by the geometric constraints of the environment and agents' rationality. In contrast, the braid group represents the set of distinct modes that could describe the collective motion of navigating agents, that is, the strategies in which they could solve the multiagent collision-avoidance problem they are about to engage in. Interestingly, while braids represent a qualitative way of modeling collision-avoidance strategies, they are able to provide sufficient detail to enable safe navigation. Explicitly reasoning about collision-avoidance strategies via braids enables a rational agent to anticipate the effect of its actions on system behavior.

Our policy outputs local actions of global outlook that contribute towards reducing uncertainty over the emerging mode. Collectively, this results in *coordination without explicit communication*, which is reflected in the reduced collision frequency of *braids | unknown paths* and *braids | known paths* algorithms. To illustrate this point, Figure 16 depicts a comparative qualitative example of the behaviors generated by our policy. For the same experiment from the 4-agent *Straight*, we observe that *braids | unknown paths* agents (Figure 16(a)) quickly converge to a clear order of intersection crossings as a result of their proactive decision-making. On the other hand, *no braids | unknown paths*

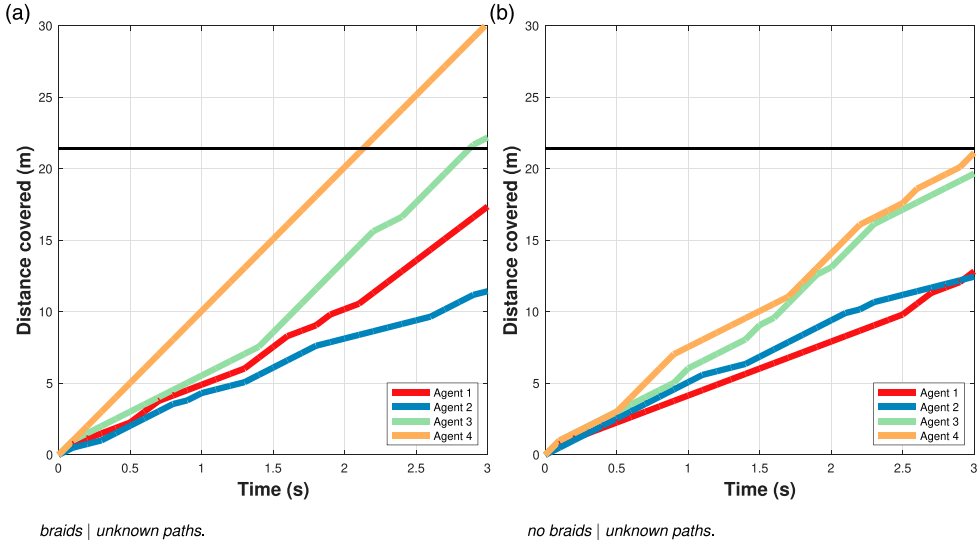

Figure 16. Distance covered per agent over the first 3*s* of execution within a 4-agent experiment under the *braids | unknown paths* and *no braids | unknown paths* conditions in the *Straight* scenario. The black line indicates arrival at the intersection.

agents (Figure 16(b)), lacking the ability of modeling the complex multiagent dynamics, appear unable to coordinate their crossings and end up colliding.

6.5.2. Coordination despite different representations. One interesting observation from our experiments is that our agents (*braids* | *unknown paths*) generally manage to coordinate collision-free intersection crossings even though they use different braid representations: each agent represents a space of modes by considering a different braid projection plane (their local $\widehat{x}$-$\widehat{t}$plane) which is unknown to others. This indicates that agents converge to the underlying multiagent behavior topology through our inference mechanism, even though they tend to use a different *language* to represent the same topological events. In other words, our mechanism enables agents to converge to the same topological structure despite looking at the scene from a different perspective and modeling the world as a conjugate braid, as discussed in Sec 3.5.

6.5.3. Coordination despite noisy behavior models. Another observation worth noting is that agents do not know the true speed preferences of others; they only maintain a noisy estimate. Despite that fact, they are able to avoid collisions to a significant extent by following the collaborative probabilistic approach of rejecting unsafe intersection traversals of equation (14).

6.5.4. Grounded experimental setup. Our evaluation was based on simulated scenarios that were grounded on the report of Najm et al. (2007) on the description of road traffic scenarios of high severity. These scenarios give rise to some of the most challenging types of multiagent interaction that can be frequently encountered by autonomous vehicles. The topological analysis of traffic behavior exhibited in simulations of these scenarios confirmed their severity (see Table 5).

7. Discussion

In this article, we presented a unified discussion of our framework making use of topological braids as an abstraction for modeling and reasoning in traffic scenes. We saw that the formalism of braids can be a valuable abstraction to extract insights about the complexity and interactivity of vehicles in a road environment like an intersection or a roundabout. Building on this finding, we proceeded to demonstrate how braids may also be a valuable representation basis for inference and decision-making. Our results showed that topological clustering of multiagent behavior may allow non-communicating agents to coordinate the traversal of challenging domains like busy intersections.

7.1. Implications

As we showed in Section 4, topological braids may formally capture critical multiagent interaction events across complex real-world traffic scenes with no explicitly specified domain knowledge. Often, the task of behavior prediction in driving domains is cast as an instance of multiagent trajectory forecasting (Salzmann et al. 2020). Understanding the support of a dataset over the space of behavior is essential in ensuring robust performance under real-world settings. Topological representations like braids could serve as valuable features to complement geometric ones, enabling a deeper understanding of the type of behavior contained in a dataset. This may be particularly useful for constructing balanced training sets, analyzing or collecting new datasets, and developing benchmarks for prediction and control.

In terms of inference, our findings from Section 1 illustrate that the principled domain knowledge induced by the braid abstraction of multiagent interaction may enable superior performance than baselines reasoning directly in the vast space of Euclidean-space trajectories. Guided by the presented insights, we see the value of topological representations like braids to be relevant to the areas of behavior prediction and decision-making for multiagent navigation by helping incorporate a global abstraction of multiagent interaction that could help improve performance. For instance, the work of Roh et al. (2020) provides an illustration of how topological signatures in the form of winding numbers may improve detailed trajectory prediction via graph neural networks; combining the symbolic expressiveness of topological braids with such an architecture could likely yield further improvements in prediction and control. Beyond that, we anticipate that reasoning about the spatiotemporal topology of multiagent behavior could likely improve the performance of belief-space approaches (Bouton et al. 2017) or reinforcement learning techniques (Isele et al. 2018) in traffic scenarios.

7.2. Limitations

7.2.1. Simulated setup. Our insights on intersection traversals are based on experiments conducted under the simulated setup of Section 1. While this setup is grounded on relevant scenarios from the typology of Najm et al. (2007), it still leaves out elements of real-world complexity such as cyclists, pedestrians, or human-controlled vehicles. The behavior models considered were meant to emulate the complexity of interacting with agents following different models. However, an important next step would be to demonstrate our framework on more realistic setup, that is, considering realistic simulators like CARLA (Dosovitskiy et al. 2017), driving datasets like the ones used in our analysis (Bock et al. 2020, 2021; Krajewski et al. 2020), and even real-world deployment on hardware like miniature racecars (Srinivasa et al. 2019).

7.2.2. Behavior models. Further, our main decision-making mechanism of Section 5 was implemented via several modeling decisions detailed in Section 6 based on insights from prior work (Mavrogiannis and Knepper 2019, 2021;

Mavrogiannis et al. 2022b). While our goal in this paper was to provide a demonstration of the value of topological features for inference and control, using simplified models, these models could be enhanced to capture behavior modeling more accurately using data-driven techniques (Roh et al. 2020; Mavrogiannis et al. 2017).

7.2.3. Beyond topological features. Abstractions like braids highlight topological patterns of interaction like vehicles' crossings or overtaking maneuvers through projection transforms or simplification rules like equation (2). However, they do not represent other geometric features, like the temporal spacing between vehicles or a driver's erratic maneuvers. These artifacts could be relevant to traffic analysis. Thus, the proposed framework is not meant to replace existing, geometry-focused tools but rather to complement them.

7.2.4. Parameter selection. Our goal in this study was to demonstrate that tools from braid theory can be valuable for the analysis of multiagent behavior in traffic scenes. In doing so, we made decisions about several parameters (e.g., see Tables 1,2,4,5). These could be adapted to the specific context of a scene or tuned as needed for particular investigations.

Declaration of conflicting interests

The author(s) declared no potential conflicts of interest with respect to the research, authorship, and/or publication of this article.

Funding

The author(s) disclosed receipt of the following financial support for the research, authorship, and/or publication of this article: This work was (partially) funded by the National Science Foundation NRI (#2132848) and CHS (#2007011), DARPA RACER (#HR0011-21-C-0171), the Office of Naval Research (#*N*00014-17-1-2617-P00004 and #2022-016-01 UW), and Amazon.

ORCID iD

Christoforos Mavrogiannis https://orcid.org/0000-0003-4476-1920

References

Alcorn MA and Nguyen A (2021) Baller2vec: A multi-entity transformer for multi-agent spatiotemporal modeling. Available at: https://arxiv.org/abs/2102.03291

Artin E (1947) Theory of braids. *Annals of Mathematics* 48(1): 101–126.

Bandyopadhyay T, Won KS, Frazzoli E, et al. (2013) Intention-aware motion planning. In: E Frazzoli, T Lozano-Perez, N Roy, et al. (eds), *Proceedings of the International Workshop on the Algorithmic Foundations of Robotics (WAFR)*. Heidelberg, Germany: Springer, pp. 475–491

Bansal M, Krizhevsky A and Ogale A (2018) *Chauffeurnet: Learning to Drive by Imitating the Best and Synthesizing the Worst*. Proceedings of Robotics: Science and Systems (RSS).

Berger MA (2001) Hamiltonian dynamics generated by Vassiliev invariants. *Journal of Physics A: Mathematical and General* 34(7): 1363–1374.

Bhattacharya S and Ghrist R (2018) Path homotopy invariants and their application to optimal trajectory planning. *Annals of Mathematics and Artificial Intelligence* 84: 139–160.

Bian Y, Li SE, Ren W, et al. (2020) Cooperation of multiple connected vehicles at unsignalized intersections: distributed observation, optimization, and control. *IEEE Transactions on Industrial Electronics* 67(12): 10744–10754.

Bock J, Krajewski R, Moers T, et al. (2020) The ind dataset: a drone dataset of naturalistic road user trajectories at German intersections Proceedings of the IEEE Intelligent Vehicles Symposium, Las Vegas, NV, USA, 19 October 2020 - 13 November 2020, pp. 1929–1934.IV

Bock J, Vater L, Krajewski R, et al. (2021) Highly accurate scenario and reference data for automated driving. *ATZ worldwide* 123(5): 50–55.

Bombara G, Vasile CI, Penedo F, et al. (2016) A decision tree approach to data classification using signal temporal logic Proceedings of the 19th International Conference on Hybrid Systems: Computation and Control, 12 - 14 April 2016, Vienna, Austria, pp. 1–10.

Bouton M, Cosgun A and Kochenderfer MJ (2017) Belief state planning for autonomously navigating urban intersections. Proceedings of the IEEE Intelligent Vehicles Symposium, Redondo Beach, CA, 11-14, June 2017, pp. 825–830

Boyland P (1994) Topological methods in surface dynamics. *Topology and Its Applications* 58(3): 223–298.

Bozga M and Sifakis J (2022) Correct by Design Coordination of Autonomous Driving Systems. *Proceedings of the International Symposium on Leveraging Applications of Formal Methods*. Springer Nature Switzerland, 13–29.

Buckman N, Pierson A, Schwarting W, et al. (2019) Sharing is caring : socially-compliant autonomous intersection negotiation Proceedings of the IEEE/RSJ International Conference on Intelligent Robots and Systems (IROS), Macau, China, 03-08 November 2019

Cao C, Trautman P and Iba S (2019) Dynamic channel: a planning framework for crowd navigation 2019 International Conference on Robotics and Automation (ICRA), pp. 5551–5557.

Caesar H, Bankiti V, Lang AH, et al. (2020) Nuscenes: A Multimodal Dataset for Autonomous Driving. *Proceedings of the IEEE/CVF Conference on Computer Vision and Pattern Recognition (CVPR)*. IEEE, 11618–11628.

Cao M, Cao K, Yuan S, et al. (2023a) Path planning for multiple tethered robots using topological braids. *Proceedings of Robotics: Science and Systems (RSS)*.

Cao M, Cao K, Yuan S, et al. (2023b) Neptune: nonentangling trajectory planning for multiple tethered unmanned vehicles. *IEEE Transactions on Robotics* 1: 1–19. DOI: 10.1109/TRO.2023.3264950

Carmody DR and Sowers RB (2021) Topological analysis of traffic pace via persistent homology*. *Journal of Physics: Complexity* 2(2): 025007.

Chang M, Lambert J, Sangkloy P, et al. (2019) Argoverse: 3d tracking and forecasting with rich maps 2019 IEEE/CVF

Conference on Computer Vision and Pattern Recognition (CVPR), Long Beach, CA, USA, 15-20 June 2019

Chazal F and Michel B (2021) An introduction to topological data analysis: fundamental and practical aspects for data scientists. *Frontiers in Artificial Intelligence* 4: 667963.

Chen J, Yuan B and Tomizuka M (2019) Deep imitation learning for autonomous driving in generic urban scenarios with enhanced safety 2019 IEEE/RSJ International Conference on Intelligent Robots and Systems (IROS). 03-08 November 2019. Macau, China. pp. 2884–2890.

Cleac'h SL, Schwager M and Manchester Z (2020) ALGAMES: a fast solver for constrained dynamic games. *Proceedings of Robotics: Science and Systems (RSS)*.

DeCastro J, Leung K, Aréchiga N, et al. (2020) Interpretable policies from formally-specified temporal properties Proceedings of the IEEE International Conference on Intelligent Transportation Systems (ITSC), Rhodes, Greece, 20-23 September 2020: pp. 1–7.

Diaz-Mercado Y and Egerstedt M (2017) Multirobot mixing via braid groups. *IEEE Transactions on Robotics* 33(6): 1375–1385.

Ding W, Chen B, Li B, et al. (2021) Multimodal safety-critical scenarios generation for decision-making algorithms evaluation. *IEEE Robotics and Automation Letters* 6(2): 1551–1558.

Dosovitskiy A, Ros G, Codevilla F, et al. (2017) CARLA: an open urban driving simulator Proceedings of the Conference on Robot Learning (CoRL), Mountain View, CA, pp. 1–16.

Dynnikov I and Wiest B (2007) On the complexity of braids. *Journal of the European Mathematical Society* 009(4): 801–840.

Ettinger S, Cheng S, Caine B, et al. (2021) Large Scale Interactive Motion Forecasting for Autonomous Driving: The Waymo Open Motion Dataset. *Proceedings of the IEEE/CVF International Conference on Computer Vision (ICCV)*. IEEE, 9690–9699.

Fontaine MC and Nikolaidis S (2022) Evaluating human–robot interaction algorithms in shared autonomy via quality diversity scenario generation. *ACM Transactions on Human-Robot Interaction* 11(3).

Gadepally V, Krishnamurthy A and Özgüner Ü (2017) A framework for estimating long term driver behavior. *Journal of Advanced Transportation*, 2017 2017: 1–11.

Ghrist R (2001) Configuration spaces and braid groups on graphs in robotics. *AMS IP Studies in Advanced Mathematics* 24: 29–40.

Ghrist R (2007) Barcodes: the persistent topology of data. *Bulletin of the American Mathematical Society* 45: 61–76.

Grannen J, Sundaresan P, Thananjeyan B, et al. (2021) Untangling dense knots by learning task-relevant keypoints Proceedings of the Conference on Robot Learning (CoRL).

Hsu YC, Gopalswamy S, Saripalli S, et al. (2018) An mdp model of vehicle-pedestrian interaction at an unsignalized intersection Proceedings of the IEEE Vehicular Technology Conference (VTC), Chicago, IL, USA, 27-30 August 2018: pp. 1–6.

Hu J, Prandini M and Sastry S (2000) Optimal maneuver for multiple aircraft conflict resolution: a braid point of view. In: *Proceedings - IEEE Conference on Decision and Control (CDC)* 4. pp. 4164–4169

Hubmann C, Becker M, Althoff D, et al. (2017) Decision making for autonomous driving considering interaction and uncertain prediction of surrounding vehicles Proceedings of the IEEE Intelligent Vehicles Symposium, Los Angeles, CA, USA, 11-14 June 2017: p. 1671–1678.IV

Isele D, Rahimi R, Cosgun A, et al. (2018) Navigating occluded intersections with autonomous vehicles using deep reinforcement learning Proceedings of the IEEE International Conference on Robotics and Automation (ICRA), Brisbane, QLD, Australia, 21-25 May 2018: pp. 2034–2039.

Jaquier N, Liang C, Rozo L, et al. (2021) Geometry and topology in robotics: learning, optimization, planning, and control. Available at: https://sites.google.com/view/geotopo-rss2021/ (24 05 2023).

Javdani S, Admoni H, Pellegrinelli S, et al. (2018) Shared autonomy via hindsight optimization for teleoperation and teaming. *The International Journal of Robotics Research* 37(7): 717–742.

Kebria PM, Khosravi A, Salaken SM, et al. (2019) Deep imitation learning for autonomous vehicles based on convolutional neural networks. *IEEE/CAA Journal of Automatica Sinica* 7(1): 82–95.

Khayatian M, Mehrabian M, Andert E, et al. (2020) A survey on intersection management of connected autonomous vehicles. *ACM Transactions on Cyber-Physical Systems* 4(4).

Koditschek DE and Rimon E (1990) Robot navigation functions on manifolds with boundary. *Advances in Applied Mathematics* 11(4): 412–442.

Konidaris G, Kaelbling LP and Lozano-Perez T (2018) From skills to symbols: learning symbolic representations for abstract high-level planning. *Journal of Artificial Intelligence Research* 61: 215–289.

Krajewski R, Moers T, Bock J, et al. (2020) The round dataset: a drone dataset of road user trajectories at roundabouts in Germany Proceedings of the IEEE International Conference on Intelligent Transportation Systems (ITSC), Rhodes, Greece, 20-23 September 2020: pp. 1–6.

Kuefler A, Morton J, Wheeler T, et al. (2017) Imitating driver behavior with generative adversarial networks 2017 IEEE Intelligent Vehicles Symposium (IV), Los Angeles, CA, USA, 11-14 June 2017, IEEE, pp. 204–211.

Lazar DA, Pedarsani R, Chandrasekher K, et al. (2018) Maximizing road capacity using cars that influence people. *Proceedings of the IEEE Conference on Decision and Control (CDC),* Miami Beach, Florida, USA, pp. 1801–1808.

Li X, Rosman G, Gilitschenski I, et al. (2021) Vehicle trajectory prediction using generative adversarial network with temporal logic syntax tree features. *IEEE Robotics and Automation Letters* 6(2): 3459–3466.

Li C, Sifakis J, Wang Q, et al. (2023) Simulation-based Validation for Autonomous Driving Systems. *Proceedings of the ACM SIGSOFT International Symposium on Software Testing and Analysis (ISSTA)*. ACM, 842–853.

Liebenwein L, Schwarting W, Vasile CI, et al. (2020) Compositional and contract-based verification for autonomous driving on road networks. *Proceedings of the International Symposium on Robotics Research (ISRR),* Puerto Varas, Chile, 11-14 December, pp. 163–181.

Lin J and McCann J (2021) An artin braid group representation of knitting machine state with applications to validation and optimization of fabrication plans Proceedings of the IEEE International Conference on Robotics and Automation (ICRA), Xi'an, China, 30 May 2021 - 05 June 2021: pp. 1147–1153.

Lindemann L, Cleaveland M, Shim G, et al. (2022) *Safe Planning in Dynamic Environments Using Conformal Prediction*

Luo W, Park C, Cornman A, et al. (2022) JFP: joint future prediction with interactive multi-agent modeling for autonomous driving. *Proceedings of the Conference on Robot Learning (CoRL)*.

Mavrogiannis CI and Knepper RA (2019) Multi-agent path topology in support of socially competent navigation planning. *The International Journal of Robotics Research* 38(2-3): 338–356.

Mavrogiannis C and Knepper RA (2021) Hamiltonian coordination primitives for decentralized multiagent navigation. *The International Journal of Robotics Research* 40(10-11): 1234–1254.

Mavrogiannis CI, Blukis V and Knepper RA (2017) Socially competent navigation planning by deep learning of multi-agent path topologies Proceedings of the IEEE/RSJ International Conference on Intelligent Robots and Systems (IROS), Vancouver, BC, Canada, 24-28 September 2017: pp. 6817–6824.

Mavrogiannis A, Chandra R and Manocha D (2022a) B-gap: behavior-rich simulation and navigation for autonomous driving. *IEEE Robotics and Automation Letters* 7(2): 4718–4725.

Mavrogiannis C, Alves-Oliveira P, Thomason W, et al. (2022b) Social momentum: design and evaluation of a framework for socially competent robot navigation. *ACM Transactions on Human-Robot Interaction* 11(2).

Mavrogiannis C, DeCastro J and Srinivasa SS (2022c) Analyzing multiagent interactions in traffic scenes via topological braids Proceedings of the IEEE International Conference on Robotics and Automation (ICRA), Philadelphia, PA, May 23-27 2022, pp. 5806–5813.

Mavrogiannis C, DeCastro JA and Srinivasa S (2023) Implicit multiagent coordination at uncontrolled intersections via topological braids. In: SM LaValle, JM O'Kane, M Otte, et al. (eds), *Algorithmic Foundations of Robotics XV*. Cham: Springer International Publishing, pp. 368–384

McGill SG, Rosman G, Ort T, et al. (2019) Probabilistic risk metrics for navigating occluded intersections. *IEEE Robotics and Automation Letters* 4(4)

Miculescu D and Karaman S (2019) Polling-systems-based autonomous vehicle coordination in traffic intersections with no traffic signals. *IEEE Transactions on Automatic Control* 65(2)

Mohammadinejad S, Deshmukh JV, Puranic AG, et al. (2020) Interpretable classification of time-series data using efficient enumerative techniques. *Proceedings of the International Conference on Hybrid Systems: Computation and Control,* pp. 1–10.

Murasugi K and Kurpita BI (1999) *A Study Of Braids. Mathematics and its Applications*. Berlin, Germany: Springer Netherlands.

Najm WG, Smith JD and Yanagisawa M (2007) *Pre-crash Scenario Typology for Crash Avoidance Research*. Washington, DC, USA: National Highway Transportation Safety Administration

Orthey A, Akbar S and Toussaint M (2020) Multilevel Motion Planning: A Fiber Bundle Formulation. *The International Journal of Robotics Research*. Sage.

Patil GR and Pawar DS (2016) Microscopic analysis of traffic behavior at unsignalized intersections in developing world. *Transportation Letters* 8(3): 158–166.

Patwardhan A, Murai R and Davison AJ (2023) Distributing collaborative multi-robot planning with Gaussian belief propagation. *IEEE Robotics and Automation Letters* 8(2): 552–559.

Pellegrini S, Ess A, Schindler K, et al. (2009) You'll never walk alone: modeling social behavior for multi-target tracking Proceedings of the IEEE International Conference on Computer Vision (ICCV), Kyoto, Japan, 29 September 2009 - 02 October 2009: pp. 261–268.

Pierson A, Schwarting W, Karaman S, et al. (2018) Navigating congested environments with risk level sets Proceedings of the IEEE International Conference on Robotics and Automation (ICRA), Brisbane, QLD, Australia, 21-25 May 2018: pp. 5712–5719.

Pokorny FT, Hawasly M and Ramamoorthy S (2016) Topological trajectory classification with filtrations of simplicial complexes and persistent homology. *The International Journal of Robotics Research* 35(1-3): 204–223.

Puranic AG, Deshmukh JV and Nikolaidis S (2021) Learning from demonstrations using signal temporal logic in stochastic and continuous domains. *IEEE Robotics and Automation Letters* 6(4): 6250–6257.

Rodriguez A, Mason MT and Ferry S (2012) From caging to grasping. *The International Journal of Robotics Research* 31(7): 886–900.

Roh J, Mavrogiannis C, Madan R, et al. (2020) Multimodal trajectory prediction via topological invariance for navigation at uncontrolled intersections. *Proceedings of the Conference on Robot Learning (CoRL)* 2216–2227.

Sadigh D, Sastry S, Seshia SA, et al. (2016) Planning for autonomous cars that leverage effects on human actions Proceedings of Robotics: Science and Systems (RSS), AnnArbor, MI, USA, June 2016

Sadigh D, Landolfi N, Sastry SS, et al. (2018) Planning for cars that coordinate with people: leveraging effects on human actions for planning and active information gathering over human internal state. *Autonomous Robots* 42(7): 1405–1426.

Salzmann T, Ivanovic B, Chakravarty P, et al. (2020) Trajectron++: dynamically-feasible trajectory forecasting with heterogeneous data. *Proceedings of the European Conference on Computer Vision (ECCV)* 683–700.

Schulz J, Hirsenkorn K, Löchner J, et al. (2017) Estimation of collective maneuvers through cooperative multi-agent planning. In: Proceedings of the IEEE Intelligent Vehicles Symposium, IV 2017, Los Angeles, CA, USA, June 11-14, 2017. pp. 624–631.

Sezer V, Bandyopadhyay T, Rus D, et al. (2015) Towards autonomous navigation of unsignalized intersections under uncertainty of human driver intent Proceedings of the IEEE/

RSJ International Conference on Intelligent Robots and Systems (IROS), Hamburg, Germany, 28 September 2015 - 02 October 2015: pp. 3578–3585.

Shalev-Shwartz S, Shammah S, Shashua A, et al. (2016) Safe, Multi-Agent, Reinforcement Learning for Autonomous Driving. *arXiv:1610.03295*. arXiv.

Srinivasa SS, Lancaster P, Michalove J, et al. (2019) *MuSHR: A Low-Cost, Open-Source Robotic Racecar for Education and Research*

Tang YC and Salakhutdinov R (2019) Multiple futures prediction. *Advances in neural information processing systems (NeurIPS)*. Curran Associates, 32.

Thiffeault JL (2010) Braids of entangled particle trajectories. *Chaos* 20(1): 017516.

Thiffeault JL (2022) Braids and Dynamics. *Springer Nature*, 9.

Thiffeault JL and Budisic M (2013) Braidlab: A Software Package for Braids and Loops. *arXiv:1410.0849 [math.GT]*. arXiv.

Tian R, Li N, Kolmanovsky I, et al. (2022) Game-theoretic modeling of traffic in unsignalized intersection network for autonomous vehicle control verification and validation. *IEEE Transactions on Intelligent Transportation Systems* 23(3): 2211–2226.

Tolstaya E, Mahjourian R, Downey C, et al. (2021) *Proceedings of the IEEE International Conference on Robotics and Automation (ICRA)*. IEEE, 3473–3479.

Tovar B, Cohen F, Bobadilla L, et al. (2014) Combinatorial filters: sensor beams, obstacles, and possible paths. *ACM Transactions on Sensor Networks* 10(3).

Vazquez-Chanlatte M, Deshmukh JV, Jin X, et al. (2017) Logical clustering and learning for time-series data, *Computer Aided Verification*. In: Proceedings of the Computer Aided Verification: 29th International Conference, CAV 2017, Heidelberg, Germany, July 24-28, 2017. Springer, pp. 305–325.

Wang W, Wang L, Zhang C, et al. (2022a) Social interactions for autonomous driving: a review and perspectives. *Foundations and Trends in Robotics* 10(3-4): 198–376. DOI: 10.1561/2300000078.

Wang W, Zhang W, Zhu J, et al. (2022b) Understanding v2v driving scenarios through traffic primitives. *IEEE Transactions on Intelligent Transportation Systems* 23(1): 610–619.

Wen TH, Chin WCB and Lai PC (2017) Understanding the topological characteristics and flow complexity of urban traffic congestion. *Physica A: Statistical Mechanics and Its Applications* 473: 166–177.

Xiaolong Wang SB and Sahin ALP (2022) Coordination-free Multi-Robot Path Planning for Congestion Reduction Using Topological Reasoning. *Journal of Intelligent & Robotic Systems*. 3rd ed. Springer Nature, 108.

Yan M, Li G, Zhu Y, et al. (2020) Learning topological motion primitives for knot planning Proceedings of the IEEE/RSJ International Conference on Intelligent Robots and Systems (IROS), pp. 9457–9464.

Yao D, Zhang C, Zhu Z, et al. (2017) Trajectory clustering via deep representation learning 2017 International Joint Conference on Neural Networks (IJCNN), Anchorage, AK, USA, 14-19 May 2017. IEEE, pp. 3880–3887.

Yue M, Li Y, Yang H, et al (2019) Detect: deep trajectory clustering for mobility-behavior analysis. In: Proceedings of the 2019 IEEE International Conference on Big Data (Big Data). Los Angeles, CA, USA, 9988-12997 September *2019*. IEEE, pp. 988–997.

Zanardi A, Zardini G, Srinivasan S, et al. (2022) Posetal games: efficiency, existence, and refinement of equilibria in games with prioritized metrics. *IEEE Robotics and Automation Letters* 7(2): 1292–1299.